European Journal of Radiology 145 (2021) 109943

Contents lists available at ScienceDirect

European Journal of Radiology

journal homepage: www.elsevier.com/locate/ejrad

Methodology, clinical applications, and future directions of body composition analysis using computed tomography (CT) images: A review

Antti Tolonen [a,*], Tomppa Pakarinen [a,b], Antti Sassi [a,b], Jere Kyttä [a], William Cancino [c], Irina Rinta-Kiikka [a,b], Said Pertuz [c], Otso Arponen [a,b]

[a] Faculty of Medicine and Health Sciences, Tampere University, Kauppi Campus, Arvo Ylpön katu 34, 33520 Tampere, Finland
[b] Department of Radiology, Tampere University Hospital, Elämänaukio, Kuntokatu 2, 33520 Tampere, Finland
[c] Connectivity and Signal Processing Group, Universidad Industrial de Santander, Cl. 9 #Cra 27, Bucaramanga, Colombia

ARTICLE INFO

Keywords:
Computed tomography
Body composition
Body composition analysis
Sarcopenia

ABSTRACT

Purpose of the review: We aim to review the methods, current research evidence, and future directions in body composition analysis (BCA) with CT imaging.
Recent findings: CT images can be used to evaluate muscle tissue, visceral adipose tissue (VAT), and subcutaneous adipose tissue (SAT) compartments. Manual and semiautomatic segmentation methods are still the gold standards. The segmentation of skeletal muscle tissue and VAT and SAT compartments is most often performed at the level of the 3rd lumbar vertebra. A decreased amount of CT-determined skeletal muscle mass is a marker of impaired survival in many patient populations, including patients with most types of cancer, some surgical patients, and those admitted to the intensive care unit (ICU). Patients with increased VAT are more susceptible to impaired survival / worse outcomes; however, those patients who are critically ill or admitted to the ICU or who will undergo surgery appear to be exceptions. The independent significance of SAT is less well established. Recently, the roles of the CT-determined decrease of muscle mass and increased VAT area and epicardial adipose tissue (EAT) volume have been shown to predict a more debilitating course of illness in patients suffering from severe acute respiratory syndrome coronavirus 2 (COVID-19) infection.
Summary: The field of CT-based body composition analysis is rapidly evolving and shows great potential for clinical implementation.

1. Introduction

The general understanding of the clinical significance of sarcopenia and cachexia is still evolving. Sarcopenia is characterized as a progressive syndrome in which there is a decrease of muscle mass and strength, whereas cachexia is a syndrome associated with a severe loss of body weight, fat, and muscle due to an underlying illness [1–4,5]. These two multifactorial conditions are independent of each other, although they may occur simultaneously in elderly people [3]. Sarcopenia and cachexia have been associated with an impaired quality of life [6,7], increased hospitalization rates [6,8] and premature mortality [6,9,10] in several diseases. At present, the principal way to treat patients with sarcopenia is to increase their physical activity, and the roles of nutritional and pharmacological interventions are being investigated [1]. Cachexia treatments may vary on the basis of the underlying disease. Nutritional counselling and pharmacological treatments (e.g. short-term use of corticosteroids) are endorsed by the American and European oncological societies in the treatment of cancer-related cachexia; however, these two guidelines have differing standpoints on the role of physical exercise [11,12].

Body composition analysis (BCA) methods are of clinical importance because before one can initiate interventions for sarcopenia or cachexia, one must diagnose their presence. Currently, computed tomography (CT) and magnetic resonance imaging (MRI) are regarded as the most accurate methods available for conducting a body composition analysis (BCA) [13]. Other methods, such as densitometry, bioimpedance analysis, and dual-energy X-ray absorptiometry, are beyond the scope of this review. (One could refer to the work of Fosbøl [14] and Albano [15] for a detailed overview of this subject.) In addition to their superior accuracy, both CT and MRI make it possible to obtain a detailed evaluation of individual skeletal muscles and muscle and adipose tissue compartments. However, routine clinical use of CT and MRI imaging in

* Corresponding author.
E-mail address: antti.h.tolonen@tuni.fi (A. Tolonen).

https://doi.org/10.1016/j.ejrad.2021.109943
Received 15 May 2021; Received in revised form 6 August 2021; Accepted 24 August 2021
Available online 30 August 2021

evaluating body composition metrics as surrogates for sarcopenia and adiposity is hindered by these methods' high costs, limited availability [5], and substantial radiation dose in the case of CT [14]. However, CT and MRI images that have been acquired for other medical purposes can be used opportunistically to assess body composition [14,16]. This review focuses on the evolving field of computer-assisted evaluation and the clinical applications of CT-based BCA. Furthermore, the article discusses the CT-based evaluation of sarcopenic obesity and epicardial adipose tissue because these subjects are of increasing clinical and research interest [1,17,18]. Given the already broad scope of this review, this article does not examine the clinical significance of intra- and intermuscular fat compartments or Hounsfield unit attenuation in muscle and fat tissue compartments.

2. Considerations of methodology

2.1. Basics of computed tomography in the context of BCA

Generally, CT images are represented as two-dimensional (2D) stacks, which is an intuitive way to inspect and analyze volumetric data on a 2D screen. Although MRI can produce true 3D data, standard CT is essentially a sequential, unidimensional 1D imaging method. In early CT scanners (step-and-shoot scanners), each 1D projection was collected sequentially in a single plane, and the images were then reconstructed into transaxial 2D slices, for which beam collimation defined the slice thickness. On the other hand, newer generations of helical CT scanners collect data by continuously moving a patient through the gantry, resulting in a helical acquisition. The 2D transaxial slices can then be reconstructed through interpolation because the acquired projections are not located in the same plane [19]. In other words, this process transforms sets of unidimensional projections into series of 2D images with a finite thickness. Thus, 2D BCA can be readily performed from a single slice (Fig. 1), and it is possible to reconstruct BCA volumes by analyzing a stack of images [20]. In practice, all modern CT scan technology is currently based on multislice (MS) technology, usually combined with helical acquisition [21]. The nMS detector composition extends the single transversal detector row in the z-direction (head-feet) to a detector array. In this way, a single scanner rotation can acquire N slices, where N is the number of detector rows, which explains the name "multislice". MS-CT has multiple advantages over the single slice-technology, including reduced tube heating, faster imaging, sub-millimeter and isotropic multiplanar reconstructions (MPR), and larger scan volumes [21,22].

Another addition to modern CT equipment is dual-energy CT (DECT) technology. In DECT, the rotating gantry consists either of two X-ray tubes separated by 90 degrees, frequency selective detectors, or a single tube in which voltage can be varied and toggled during the scan sequence [23]. This technology is based on a material's frequency-dependent attenuation properties, especially variations between the differences in the attenuation spectra of different materials, such as iodine and bone. For example, dual-source DECT acquires two sets of data, which can be weighted to create a single composite image, material decomposition images [23,24], or effective atomic number maps with high temporal resolution [25]. Additionally, dual-source DECT facilitates faster acquisition, which could be beneficial in processes such as gated cardiac imaging, because two orthogonal sources require a quarter of a rotation for reconstruction instead of the 180 degrees necessary with a single source [19]. For such reasons, DECT has been adopted in a growing number of applications and is currently utilized in different forms of clinical imaging, including abdominal, urinary, and vascular imaging [24,26].

2.2. Definition of Hounsfield units (HU) and the role of applied HU ranges in BCA

The image data in CT imaging is collected as attenuated X-ray projections, which are reconstructed as stacks of 2D images. Next, the CT images are presented on a computer screen with grayscale values, which correspond to HU values defined as follows:

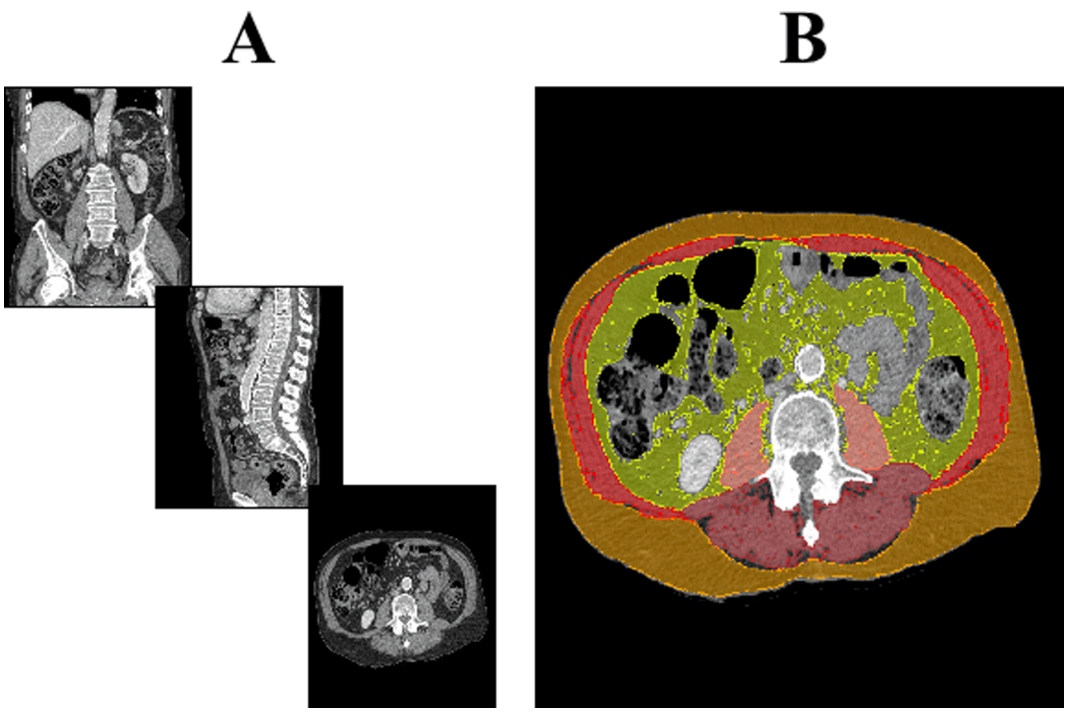

Fig. 1. An example of the workflow used to determine skeletal muscle mass and visceral and subcutaneous adipose tissue compartments at the level of the 3rd lumbar vertebra. A) The axial plane level is determined with reference to the coronal and sagittal views. B) Hounsfield unit (HU) ranges (e.g., from −190 to −30 and −29 to 150) are applied to facilitate the definition of the visceral and subcutaneous adipose tissue and the skeletal muscle areas. Undesired tissues (such as the bowel) and external structures (such as the couch) with overlapping HU values are manually removed.

$$HU_x = (\mu_x - \mu_{water})/(\mu_{water} - \mu_{air}) \quad (1)$$

where μ is the linear attenuation coefficient for a given material defined as shown here:

$$\mu_x = T^{-1}\ln(I_0/I) \quad (2)$$

where τ is the material thickness, I is the transmitted intensity, and I_0 is the initial intensity. The Hounsfield units are useful in depicting X-ray attenuation because the values are relative to physical material attenuation properties, i.e. water and air. This association of X-ray attenuation means that HU values can be used to differentiate between tissue types [27,22,28–31]. However, the sole use of HUs as absolute measures in tissue identification is not possible, as HU values overlap between tissues with similar attenuation properties. Furthermore, there are numerous types of CT artefacts, a slight dependence between HU values and tube voltage, reconstruction algorithms being used, and variable energy imaging; these all complicate the effective diagnostic application of HU values [32]. These problems could be partially corrected by standardizing the measured HU values with a known tissue. For example, HU drifting may be corrected with an arterial blood density standardization in lung densitometry [33], and cerebrospinal fluid mean HU subtraction has been suggested when attempting to differentiate between white and grey matter [34].

HU values facilitate the segmentation of the tissues of interest in BCA, meaning adipose and muscle tissues [22,28–31]. Adipose tissue is classically segmented into two compartments: the subcutaneous and visceral adipose tissue compartments (SAT and VAT compartments, respectively) [35]. The HU range for adipose tissue is broad, and several ranges (e.g., −200 to −30 [36,37], −190 to −30 [22], and −195 to −45 [28]) have been proposed. The subcutaneous fat tissue compartment may cover a slightly different HU range than that of VAT (i.e. −190 to −30 and −150 to −50, respectively) [29]. Consistently, Rosenquist et al. reported a small (2.1 HU value) difference in mean standard deviations between the two different compartments (SAT (7.6 HU values) and VAT (5.5 HU values)) [28]. Nevertheless, the spatial location is a descriptive segmentation feature distinguishing between VAT and SAT (Fig. 1). HU values of muscle and lean tissues are higher than those of adipose tissue. The HU values of muscle tissue in BCA are typically set to begin above the highest HU value used to analyze adipose tissue and range up to an HU value of 150 [29,30].

2.3. 2D and 3D measurements and the applied cut-off values for CT-based body composition metrics

As previously discussed, the skeletal muscle tissue and VAT and SAT compartments are of interest in CT-based BCA [4,5,6,21,22]. Single-slice CT-based BCA measurements display good agreement with single-slice MRI measurements [38–41]. Single-slice MRI BCA metrics correlate well with whole-body MRI-metrics [42,43]. When approximating the total volumes of these tissues, the most widely accepted level at which to perform 2D measurements is the 3rd lumbar vertebra (L3) (see Figs. 2 and 3; Tables 1 and 2) [44]. Other levels at which the single-slice BCA measurements have been measured include the cervical spine (especially the 3rd cervical vertebra) [45], the 12th thoracic vertebra [46], other lumbar vertebrae [44], and various levels of the thigh [44]. Anatomical landmarks, such as the vertebrae and other bony structures, are used as boundaries when performing volumetric measurements of adipose and muscle tissue compartments. The boundaries used for volumetric analyses include the areas between the 2nd lumbar vertebra and the sacrum [47]; the 12th thoracic vertebra and the superior aspect of the femoral head for adipose tissue [48]; the 12th thoracic vertebra and the inferior surface of the 1st sacral vertebra for the determination of the paraspinal muscles [48]; the 10th thoracic vertebra and the 5th lumbar vertebra [49]; and the 1st and the 5th lumbar vertebra [50]. However, the literature lacks studies comparing the performances of different levels used for 2D single-slice BCA and volumes used for BCA in the evaluation of the likelihood of different outcomes in different diseases.

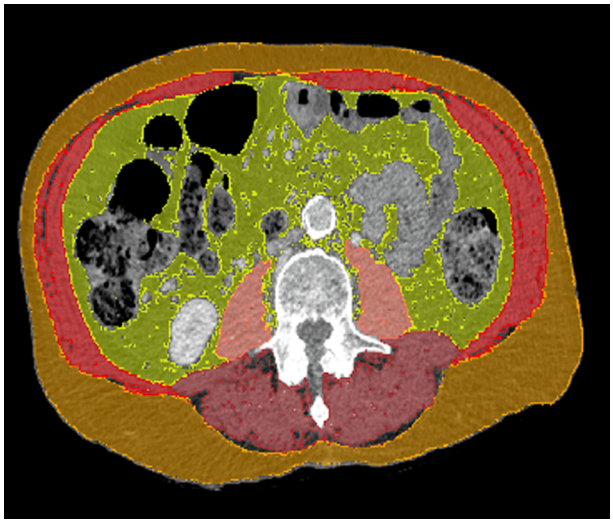

Fig. 2. Two-dimensional body composition metrics evaluated at the level of the 3rd lumbar vertebra. The psoas (pink), the paraspinal muscles and quadratus lumborum (dark red), and the rectus abdominis and the obliques (bright red) are often quantified together (i.e. as the total muscle area). Visceral adipose tissue (yellow) and subcutaneous adipose tissue (orange) compartments can be readily characterized separately. (For interpretation of the references to color in this figure legend, the reader is referred to the web version of this article.)

The cut-off values for single-slice CT-based surrogates describing sarcopenia and VAT and SAT compartments remain to be standardized. The cut-off values for CT-based surrogates for sarcopenia vary in the literature on the bases of gender, the level used for BCA evaluation, and the evaluated muscle or muscle compartment [44]. Thus, instead of presenting crude muscle areas, researchers often normalize muscle areas with respect to a patient's height [44], resulting in the assessment of a value called the skeletal muscle index (SMI) (Eq. (3)).

$$SMI = Skeletal\ muscle\ area / Height^2 \quad (3)$$

There are several SMI cut-off points for defining surrogate measurements for sarcopenia based on gender, BMI, muscle group, and the level used for the analysis [17–21,44,51]. For instance, the recent meta-analysis of Amini et al. [44] concluded that the most common cut-off values for SMI calculated at the L3 level using the total abdominal wall area range between 52 and 55 cm^2/m^2 for men and between 39 and 41 cm^2/m^2 for women. Furthermore, differing VAT cut-off values have been proposed, such as those ranging between 124.3 and 163.8 cm^2 for men and between 80.1 and 173.0 cm^2 for women (e.g., [52–54]). There appears to be no consensus on cut-off values for SAT or volumetric measurements.

2.4. Computer-aided diagnostics and artificial intelligence

An area delineation of tissue compartments in single slices is straightforward and does not necessarily require automatic analysis or processing tools. However, manual outlining of the boundaries of different tissue compartments means that the analyses are subjected to inter-reader variability. Furthermore, the large number of slices (typically hundreds) means that manual 3D BCA is time-consuming. A greater exploitation of computer-assisted diagnostic (CAD) tools could stimulate more BCA research, and a greater availability of CAD tools could help move BCA to clinics.

The current CAD tools for CT segmentation can be categorized as manual, semiautomatic, and automatic tools (Table 3). Manual tools

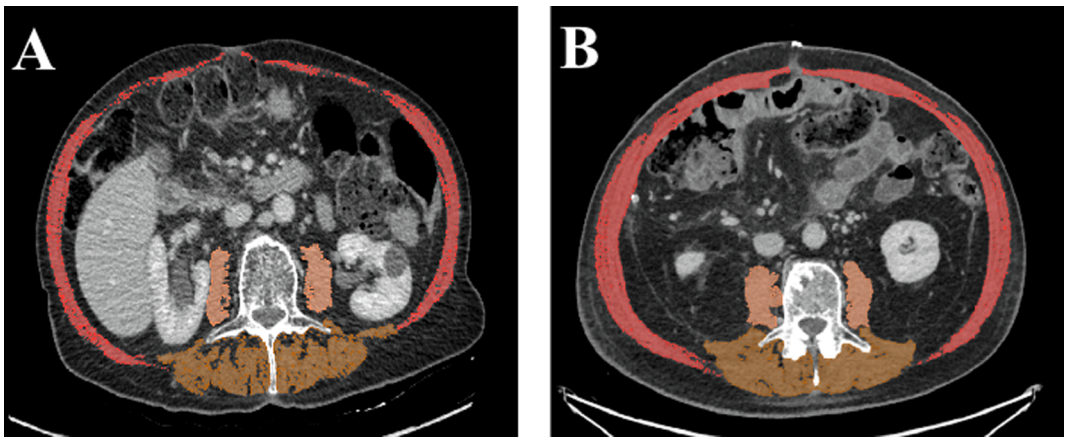

Fig. 3. The figure shows two patients with normal BMIs. The area of all the visible muscles (the psoas (pink), the paraspinal muscles and quadratus lumborum (brown), and the rectus abdominis and the obliques (red)) is first segmented and then normalized according to the patient's height to determine the skeletal muscle index (SMI). The patient with decreased muscle mass (A) has an SMI value of 24.9 cm^2/m^2, and the non-sarcopenic patient (B) has an SMI value of 50.3 cm^2/m^2. (For interpretation of the references to color in this figure legend, the reader is referred to the web version of this article.)

offer the basic capabilities for acquiring and saving manual annotations of an experienced reader [55–59]. The main difference between semi- and fully automated methods is that there is a need for user interaction to conduct the segmentation process with semiautomatic methods [60–62]. Semiautomatic methods often leverage the HU value-based thresholding and require manual correction [63,55,57]. Region-growing methods can be used for 2D analysis and have the added benefit of achieving a quick 3D delineation [64–66]. However, these methods are best suited for tissues in which there are clear contrasts with surrounding tissue (such as the liver); otherwise, these methods often require manual corrections after the automatic process [63]. Other methods include edge detection [67,68], atlas-based localization [69,70], various deep-learning methods, and artificial neural networks [71–74]. The use of fully automatic tools is currently limited by the variability of patient habitus [71], morphologies [75,76], and the overlapping of Hounsfield units between tissues [77]. On the other hand, it is important to distinguish two categories of CAD tools for quantitative CT-based BCA according to their access policies. These two groups are commercial and open-access tools. The main advantages of commercial tools are the support offered by developers and their customization for specific imaging and PACS systems [65,78,79,62]. Alternatively, open-access tools are freely available for research and educational purposes [55,57,56,58,66,59]. Their main advantage is that open-access tools are readily accessible to a wider userbase because they are not blocked by paywalls.

Indeed, various widely utilized tools can be applied in the analysis of CT images. Recently, artificial intelligence (AI) has emerged as a promising tool for assisting with several image analysis tasks, including semi-automated and fully-automated annotation and segmentation of images [61]. Additionally, there is a wide range of alternatives offered either as integrated bundles to PACS systems or by certain specialized software developers. Some of these tools are summarized in Table 3. In the table, the phrase "open source" refers to the availability of the source code, which facilitates its modification and customization by researchers to meet special requirements.

3. CT-derived BCA in a clinical context

3.1. CT-determined loss of skeletal muscle mass in a clinical context

The clinical significance of the CT-determined loss of skeletal muscle mass is well-established in patients with cancer and patients who are critically ill or about to undergo surgery. Beyond these, other scenarios in which the CT-determined muscle mass evaluation has been utilized are summarized in Table 1.

The CT-determined decrease in skeletal muscle mass as a surrogate for sarcopenia has been most extensively studied in patients with cancer. Indeed, decreased muscle mass correlates with decreased survival in patients with breast [80–82], prostate [83], gastrointestinal [84–90], urinary tract [91] and head and neck cancers, among others (Table 2). Furthermore, patients who undergo chemotherapy for advanced or metastatic cancers who preserve skeletal muscle mass irrespective of other important prognostic factors appear to have a better overall survival rate [92,93–95]. The accrued data suggests that patients with CT-quantified loss of skeletal muscle mass may be more susceptible to chemotherapy-related toxicities [96–101]. The association between the CT-quantified loss of muscle mass and quality of life has not been extensively studied. However, the results of these relatively small-scale studies [102,103] suggest that a CT-determined loss of skeletal muscle mass may not reduce quality of life.

Additionally, the CT-determined evaluation of the loss of skeletal muscle mass has shown promise in the evaluation of critically ill patients and patients undergoing surgery. For instance, the CT-determined loss of skeletal muscle mass at the level of the 3rd lumbar vertebra has been associated with longer hospital stays [104] and higher 30-day mortality [104–107] in patients admitted to the intensive care unit (ICU). Notably, one study found no correlation between the initial BCA parameters measured from the CT images obtained at the time of hospital admission and mortality. On the other hand, if a patient experienced a loss of fat tissue during his or her hospital stay, this occurrence increased the patient's mortality risk [108]. The loss of skeletal muscle mass was reported to predict increased mortality and length of hospital stay in trauma patients [109] and in patients with acetabular [110,111] and femoral [112–114] fractures. Moreover, several publications have highlighted that sarcopenia appears to be independently associated with increased mortality after emergency laparotomy [115–118], cardiac operations [119–121], and a longer duration of hospital stay after cardiac operations [122].

Recently, the role of a CT-determined decrease in muscle mass as a marker of sarcopenia has been evaluated as an outcome predictor in patients with COVID-19. It is frequently possible to conduct a CT-based estimation of muscle mass since patients who are hospitalized are often imaged as a part of their diagnostic work-ups. On this subject, an observational study revealed that a decreased paraspinal muscle area at the level of the 5th thoracic vertebra correlated with an increased risk of ICU admission and death in hospitalized adults and elderly COVID-19 patients (median age 65 years) who were scanned as a part of their routine care [123]. Another cohort study examining patients with a

Table 1
Role of computed tomography-determined loss of skeletal muscle mass and visceral and subcutaneous adipose tissue compartments in various clinical scenarios

	Skeletal muscle mass	References	Visceral and subcutaneous adipose tissue compartments	References
Malignancies	See Table 2.	–	See Table 2.	–
Critically ill patients	Decreased skeletal muscle mass (L3) is associated with longer hospital stays and increased mortality.	[104,105,108]	Low VAT at the time of ICU admission is associated with increased mortality.	[108]
Preoperative surgical assessment	Preoperatively determined decreased skeletal muscle mass (L3, T12) is associated with longer hospital stays and increased mortality.	[119,120,121,122]	Preoperative low VAT and SAT (umbilical level) are associated with increased mortality.	[174]
Metabolic diseases	Decreased skeletal muscle mass (L3, L4-5) is associated with an increased risk of diseases related to metabolic syndrome.	[175,176,177]	Increased VAT is associated with an increased risk of diseases related to metabolic syndrome (including atherosclerosis and coronary plaques).	[126,127,128,129,130,131,132,133,134,141,142,143,135,136,137,138,139,138,140,178]
Pulmonary diseases	Decreased skeletal muscle mass (T12, T4, above the aortic arch) is associated with increased mortality in pulmonary fibrosis.	[179,180]	Decreased SAT (above the aortic arch) is associated with an increased risk of mortality in obstructive pulmonary disease.	[181]
COVID-19	Decreased skeletal muscle mass (T5, T12, above the aortic arch) is associated with increased risks of ICU admission and death.	[123,124,125]	Increased VAT (L1, L3) is associated with increased risks of ICU admission and hospitalization.	[144,145,146]
Neurological diseases	Decreased skeletal muscle mass (L3, temporal muscle thickness, masseter muscle cross sectional area) correlates with the risk of Alzheimer's disease and brain atrophy. This factor is also associated with a lower score on the Glasgow Outcome Scale and increased mortality after traumatic brain injury (L3).	[182,183,184]	The roles of VAT and SAT remain largely unstudied.	–

T12/L1/L3/L4/L5 = measurements are performed at the level of the 12th thoracic vertebra or at the levels of the 1st, 3rd, 4th, or 5th lumbar vertebra, respectively; L4-5 = measurements are performed at the level between the 4th and 5th vertebrae; VAT = visceral adipose tissue; SAT = subcutaneous adipose tissue; ICU = intensive care unit.

median age of 62 years revealed that individuals defined as sarcopenic on the basis of their skeletal muscle index (cross-sectional muscle area measured at the level of the 12th thoracic vertebra) experienced longer hospital stays and were more likely to die from the infection [124]. In the same way, a third study confirmed that individuals with decreased pectoralis muscle areas were more likely to have longer hospital stays and die of COVID-19 [125].

3.2. CT-determined visceral and subcutaneous adiposity in clinical context

The determination of VAT with CT has shown promise in various clinical scenarios. Low visceral adiposity appears to be a marker of decreased survival and worse outcomes in patients who are critically ill, admitted to the ICU or who undergo surgery (Tables 1 and 2). Despite the relatively extensive literature on this subject, the independent roles of CT-determined SAT area and SAT volume have been less convincing (Tables 1 and 2).

Table 2
Role of computed tomography-determined loss of skeletal muscle mass and visceral and subcutaneous adipose tissue in various types of cancers

	Skeletal muscle mass	References	Visceral and subcutaneous adipose tissue compartments	References
Gynecological and breast cancers				
Ovarian	Decreased skeletal muscle mass (L3) is associated with decreased survival in patients with advanced ovarian cancer.	[95,185]	A high VAT/SAT ratio (mid-waist level) is associated with decreased survival. High SAT is associated with decreased survival.	[186,187]
Cervical	Decreased psoas muscle mass (L3) is associated with decreased survival in metastatic cervical cancer.	[188]	The roles of VAT and SAT remain unstudied.	–
Breast	Decreased skeletal muscle mass (L3, umbilical level) is associated with decreased survival in patients with early breast cancer and those with advanced breast cancer undergoing neoadjuvant chemotherapy.	[80,81,82]	High VAT (umbilical level) is associated with decreased survival in advanced breast cancer. However, high VAT (L3) is associated with increased progression-free survival in patients undergoing CDK4/6 inhibitor treatment.	[81,189]
Gastrointestinal cancers				
Esophageal	Decreased skeletal muscle mass (L3) is associated with decreased survival in gastroesophageal cancers.	[84,85,86]	A high VAT/SAT ratio (umbilical level) is associated with decreased survival.	[190]
Gastric	Decreased skeletal muscle mass (L3) is associated with decreased survival in foregut cancer and metastatic gastric cancer.	[93,94]	High VAT (umbilical level) is associated with decreased survival, and SAT is associated with increased survival in locally advanced gastric cancer.	[191]
Colorectal	Decreased skeletal muscle mass (L3) is associated with decreased survival at all stages of colorectal cancer.	[192,90]	High VAT (L3) is associated with decreased survival in metastatic colorectal cancer.	[193,194,90]
Pancreatic	Decreased skeletal muscle mass (L3) is associated with decreased survival in advanced pancreatic cancer.	[89]	High VAT (L3) is associated with decreased survival. The loss of VAT during treatment is associated with decreased survival.	[195,196]
Urogenital cancers				
Renal	Decreased skeletal muscle mass (L3) is associated with decreased survival in metastatic renal cancer.	[91]	The roles of VAT and SAT remain unstudied.	–
Prostate	Decreased skeletal muscle mass (L3) is associated with decreased survival.	[83]	High VAT (L3) is associated with decreased survival.	[83]
Other malignancies				
Lung	Progressive loss of skeletal muscle mass (L3, L2/3) during the first line of chemotherapy is associated with decreased survival.	[92,197]	A high pre-chemotherapy VAT/SAT ratio (L2-3) is associated with decreased survival.	[197]
Melanoma	Decreased skeletal muscle mass (L3) is associated with decreased survival in metastatic melanoma.	[198]	A high VAT/SAT ratio (L3-4) is associated with decreased survival in metastatic melanoma.	[199]
Head and neck	Decreased skeletal muscle mass (L3) is associated with decreased survival in patients with advanced head and neck cancers.	[200,201]	Low adipose tissue volumes (hyoid bone to the 1st rib) are associated with decreased survival.	[202]

L3 = measurements are performed at the level of the 3rd lumbar vertebra; L2-3/L3-4 = measurements are performed at the levels between the 2nd and 3rd and the 3rd and 4th vertebrae, respectively; VAT = visceral adipose tissue; SAT = subcutaneous adipose tissue.

The role of CT-quantified VAT and SAT areas is of special interest in diseases related to metabolic syndrome. For instance, the CT-quantified VAT area has been shown to be an independent risk factor for diseases related to this syndrome [126–128], such as diabetes and insulin resistance [129,130], hypertension [131–133], hyperlipidemia [134], and coronary artery and carotid atherosclerosis [135–137]. A high VAT area was associated with coronary stenosis in asymptomatic patients, independent of other cardiovascular risk factors [138], and linked with the presence of both calcified and non-calcified coronary plaques [138–140]. These previously referenced studies have reported conflicting results on the role of SAT and overall adiposity as risk factors for metabolic diseases. Thus, the association between SAT and overall adiposity and diseases related to the metabolic syndrome remains somewhat unclear [141–143]. Additionally, SAT does not seem to be a risk factor for developing coronary plaques. In fact, one study detected

Table 3
An overview of software tools used for BCA

Tool	Description	Open-source	Licence	Reference
3D Slicer	Software for visualization and analysis of medical imaging datasets. Supports commonly used datasets, such as images, segmentations, surfaces, annotations, transformations, etc., in 2D, 3D, and 4D.	Yes	Open-access	[55]
ITK Snap	A project for the development of interactive medical image processing software that can be used as a toolkit or an application framework for software development. Supports manual segmentation and semi-automatic segmentation of organs in image volumes.	Yes	Open-access	[57]
Medical Imaging Interaction Toolkit (MITK)	A tool for manual and semi-automatic segmentation of 3D medical images.	Yes	Open-access	[56]
ePAD Imaging Platform	A tool to visualize, annotate and perform quantitative analysis of radiological images. Can be used to generate regions of interest that circumscribe the targets automatically by means of segmentation plugins that use line and point annotations as seeds.	Yes	Open-access	[58]
SliceOmatic	A software developed for research on body composition, allowing measurement, segmentation, and analysis of multislice scanner data. This program facilitates semi-automatic segmentation based on thresholding, mathematical morphology, region growing, and snake operations. The software also has a module for automatic segmentation, allowing the identification and labeling of muscle areas and subcutaneous and visceral fat.	No	Commercial	[66]
ImageJ	A widely used tool by the image processing community that can be used to display, edit, analyze, process, save, and print images.	Yes	Open-access	[59]
RIL-Contour	An artificial imaging-based system that supports the use of manual, semi-automated, and deep learning methods for medical image annotation.	Yes	Open-access	[203]
OsiriX	A DICOM viewer offering advanced 2D and 3D post-processing techniques, 3D and 4D navigation, and full integration with any PACS. This tool allows manual annotation and semi-automatic annotation based on region growing.	No	Commercial	[65]
AMBRA	Supports the exchange and upload of medical images from various sources. Additionally, the AMBRA web viewer features viewing tools for image annotation along with hanging protocols and viewer customization. In this viewer, physicians can perform measurements and annotations or purchase images.	No	Commercial	[78]
SOPHiA AI	A cloud-based platform that standardizes, computes, and analyzes data from multiple modalities. It leverages patented machine learning algorithms to segment medical images, extract standardized radiomic features, and correlate them with the results.	No	Commercial	[62]
ProtonPACS	An image archiving and communications system based on Intelerad PACS software. It offers customized solutions, such as radiology PACS, orthopedic PACS, and hospital PACS.	No	Commercial	[79]
iTomography	A reconstruction software for CT imaging, CT data processing, and image enhancement.	No	Commercial	[204]
Syngo.via	A software for 3D reading and advanced visualization. Based on a client–server architecture, multimodal images can be accessed and processed anywhere.	No	Commercial	[205]

2D = two-dimensional; 3D = three-dimensional; 4D = four-dimensional; CT = computed tomography.

an inverse relationship between the SAT area and the risk of plaques [140].

The CT-quantified VAT seems to have prognostic value in patients with COVID-19 infections. One study found that in these patients, increased VAT was associated more strongly with a risk of ICU admission and mechanical ventilation than a simple measurement of abdominal circumference [144]. Notably, one study reported that although VAT and SAT were equally beneficial in predicting the

likelihood of ICU admission in a univariate analysis, VAT had the strongest correlation with this outcome in the multivariate analysis [145]. In another study, a higher L3 VAT area was also a predictor of hospitalization, unlike BMI, L3 SAT area, or L3 total adipose tissue area [146].

4. Emerging concepts: Sarcopenic obesity and the quantification of epicardial adipose tissue volume

4.1. Sarcopenic obesity

Sarcopenic obesity (SOB), the concomitant presence of sarcopenia and obesity, is a multifactorial condition that may increase the likelihood of metabolic impairment and physical disability more than either sarcopenia or obesity alone [147,148]. Studies have proposed various combinations of clinical parameters (e.g., the hand grip test and BMI) and CT-quantified BCA parameters that describe the loss of skeletal muscle mass and increased fat mass in the determination of SOB [17,148]. However, the best definition and method of choice to determine SOB remain to be established [149]. A recent review by Zhang et al. found that older patients who were deemed to have SOB based on varying definitions displayed an increased risk of all-cause mortality in comparison to those without SOB. This conclusion remained unchanged in their subgroup analyses when the loss of skeletal muscle mass and increased VAT were defined from CT images [17].

Certain studies have examined SOB defined fully or partly on the basis of CT-derived BCA metrics in several types of cancer. In a study by Prado et al. [150], SOB (sarcopenia: skeletal muscle area at the level of the 3rd lumbar vertebra < 52.4 cm^2/m^2 in men and < 38.5 cm^2/m^2 in women, obesity: BMI level ≥ 30 kg/m^2) was an independent predictor of impaired survival in patients with gastrointestinal and respiratory tract tumors. Using the same definition for sarcopenia, Tan et al. and Gruber et al. demonstrated that patients with pancreatic cancer who were overweight or obese (BMI ≥ 25 kg/m^2) had lower survival rates than those at lower BMIs [151,152]. Peng et al. found contradictory results showing that only sarcopenia (cut-offs for total muscle mass at L3 level: 42.2 cm^2/m^2 for men and 33.9 cm^2/m^2 for women) was a marker of impaired survival in patients with pancreatic adenocarcinoma, not sarcopenic obesity (obesity is defined as VAT/total adiposity ratio > 2 at the L3 level) [36]. Elderly patients with esophageal squamous cell carcinoma (ESCC) treated with neoadjuvant chemotherapy (NAC) who were affected by SOB (sarcopenia: skeletal muscle index < 42.0 cm^2/m^2 in men and < 38.0 cm^2/m^2 in women, obesity: VAT > 100 cm^2), not sarcopenia, had a lower survival rate than patients without SOB [153]. Another study with patients with ESCC and esophageal adenocarcinoma indicated that the presence of sarcopenia or sarcopenic obesity was not associated with impaired short- or long-term survival [154]. The five-year overall survival rate but not the five-year recurrence-free survival (RFS) was statistically significantly better in non-SOB than SOB patients (defined as VAT/total muscle area ratio > 3.2 at the level of the 3rd lumbar vertebra) in patients with non-metastatic rectal carcinoma [155]. Furthermore, SOB defined using the CT-derived metrics of BCA has shown promise in the prediction of all-cause mortality in patients undergoing cardiovascular surgery [156] and of mortality in trauma [157] patients.

4.2. Quantification of epicardial adipose tissue

Throughout the literature, the definitions of the anatomical fat compartments adjacent to the heart (especially epicardial adipose tissue (EAT), pericardial AT, and paracardial AT) vary. However, the epicardial fat compartment is often defined as the fat in the heart located between the myocardium and the visceral (inner) layer of pericardium [158–160]. This study briefly reviews the quantification of EAT using CT given the fact that EAT is biologically active tissue [161], and its radiological quantification has been of special interest [160] with respect to cardiovascular health [160].

The upper cut-off value for normal EAT on CT remains to be established. Dey et al. [162] showed that the values reported in the literature with various inclusion criteria varied between 125.0–139.4 cm^3 for men and 119.0–125.0 cm^3 for women. Additionally, a recent meta-analysis by Mancio et al. [163] claimed that patients with increased EAT volumes were more likely to have obstructive and significant coronary stenosis, myocardial ischemia, or major adverse cardiovascular events. However, this study revealed no association between the EAT volume and the presence of coronary calcification after adjusting for confounding factors. Furthermore, another systematic review demonstrated that atrial fibrillation (AF) was associated with increased epicardial fat volume [164], and patients with paroxysmal AF had lower EAT volumes than patients with persistent AF. Patients with chronic obstructive pulmonary disease may also have an increased amount of EAT [165,166]. Notably, recent findings have shown that patients with larger epicardial fat compartments often experience more severe COVID-19 infections [167,168] and worse outcomes (i.e., clinical deterioration or death) [169]. Additionally, such patients are more susceptible to myocardial injury [170] and the development of new-onset AF [171]. However, other studies have found no differing EAT volumes between COVID-19 survivors and those who die of the disease [172] or those who live but experience severe outcomes [173].

5. Future research

The wide implementation of CT-based BCA in clinics warrants further characterization against the clinical parameters describing sarcopenia and cachexia. Beyond this, their clinical utility must be tested against well-founded outcome parameters in different patient populations. The impacts of nutritional and exercise interventions on CT-based body composition and clinical outcomes remain largely unexplored for many diseases. Furthermore, the role of sarcopenic obesity is of growing interest and warrants further research.

Single-slice measurements performed at the level of the 3rd lumbar vertebra are viewed as the most accurate representations of true volumetric whole-body metrics. Relatively few investigators have compared the different levels used for 2D analyses and volumetric measurements in terms of how well they represent the entire body's adipose and muscle compartments and different clinical endpoints. In the same way, the use of different regions (e.g., the cervical and thoracic regions) for BCA in situations where L3 slices are unavailable requires further validation.

One fundamental aspect of BCA is the accurate segmentation of different regions in CT images. In turn, this process requires sophisticated computerized tools. Recently, studies have demonstrated that AI methods based on deep learning can achieve excellent results in the segmentation of chest and abdominal CT images. However, further development of these methods for clinical studies faces several challenges, such as the need for large, annotated datasets and evaluations of new techniques in real-life clinical settings [150].

6. Conclusions

Overall, CT and MRI images can be used to evaluate skeletal muscle and VAT and SAT compartments. Although CT inevitably exposes patients to ionizing radiation, CT-based BCA can be performed opportunistically from images obtained during a clinical work-up. Manual and semiautomatic segmentations of these body compartments are most often performed at the level of the 3rd lumbar vertebra. The decreased amount of the CT-determined skeletal muscle mass is a marker of impaired survival in many patient populations, including patients with cancer and those undergoing several types of surgery or admitted to the ICU. Additionally, patients with increased VAT are more susceptible to impaired survival and worse outcomes, although those patients who are critically ill or admitted to ICU or who undergo surgery appear to be exceptions to this rule. On the other hand, the independent significance

of SAT is less established. Recently, CT-determined decreased muscle mass and increased VAT area and EAT volume have been shown to predict more severe courses of illnesses in COVID-19 patients. The evolving field of CT-based body composition analysis shows great potential for being implemented soon into clinical practice.

CRediT authorship contribution statement

Antti Tolonen: Writing – original draft, Data curation, Validation, Writing – review & editing, Conceptualization. **Tomppa Pakarinen:** Writing – original draft, Validation, Conceptualization. **Antti Sassi:** Writing – review & editing, Conceptualization. **Jere Kyttä:** Writing – review & editing, Visualization, Validation, Conceptualization. **William Cancino:** Writing – original draft, Validation. **Irina Rinta-Kiikka:** Writing – review & editing, Supervision, Validation. **Said Pertuz:** Supervision, Validation, Writing – original draft, Writing – review & editing. **Otso Arponen:** Supervision, Writing – original draft, Writing – review & editing, Conceptualization, Project administration, Validation.

Declaration of competing interest

The authors declare that they have no known competing financial interests or personal relationships that could have appeared to influence the work reported in this paper.

Acknowledgments

We wish to thank the reviewers for their insightful comments that significantly improved the manuscript.

References

[1] A.J. Cruz-Jentoft, A.A. Sayer, Sarcopenia, Lancet (London, England) 393 (2019) 2636–2646, https://doi.org/10.1016/S0140-6736(19)31138-9.
[2] S. Ali, J.M. Garcia, Sarcopenia, cachexia and aging: diagnosis, mechanisms and therapeutic options - a mini-review, Gerontology. 60 (2014) 294–305, https://doi.org/10.1159/000356760.
[3] R.A. Fielding, B. Vellas, W.J. Evans, S. Bhasin, J.E. Morley, A.B. Newman, G. Abellan van Kan, S. Andrieu, J. Bauer, D. Breuille, T. Cederholm, J. Chandler, C. De Meynard, L. Donini, T. Harris, A. Kannt, F. Keime Guibert, G. Onder, D. Papanicolaou, Y. Rolland, D. Rooks, C. Sieber, E. Souhami, S. Verlaan, M. Zamboni, Sarcopenia: an undiagnosed condition in older adults. Current consensus definition: prevalence, etiology, and consequences. International working group on sarcopenia, J. Am. Med. Dir. Assoc. 12 (2011) 249–256, https://doi.org/10.1016/j.jamda.2011.01.003.
[4] W.J. Evans, J.E. Morley, J. Argilés, C. Bales, V. Baracos, D. Guttridge, A. Jatoi, K. Kalantar-Zadeh, H. Lochs, G. Mantovani, D. Marks, W.E. Mitch, M. Muscaritoli, A. Najand, P. Ponikowski, F. Rossi Fanelli, M. Schambelan, A. Schols, M. Schuster, D. Thomas, R. Wolfe, S.D. Anker, Cachexia: a new definition, Clin. Nutr. 27 (2008) 793–799, https://doi.org/10.1016/j.clnu.2008.06.013.
[5] E. Marty, Y. Liu, A. Samuel, O. Or, J. Lane, A review of sarcopenia: Enhancing awareness of an increasingly prevalent disease, Bone. 105 (2017) 276–286, https://doi.org/10.1016/j.bone.2017.09.008.
[6] J. Giglio, M.A. Kamimura, F. Lamarca, J. Rodrigues, F. Santin, C.M. Avesani, Association of sarcopenia with nutritional parameters, quality of life, hospitalization, and mortality rates of elderly patients on hemodialysis, J. Ren. Nutr. Off. J. Counc. Ren. Nutr. Natl. Kidney Found. 28 (2018) 197–207, https://doi.org/10.1053/j.jrn.2017.12.003.
[7] S. Schwarz, O. Prokopchuk, K. Esefeld, S. Gröschel, J. Bachmann, S. Lorenzen, H. Friess, M. Halle, M.E. Martignoni, The clinical picture of cachexia: a mosaic of different parameters (experience of 503 patients), BMC Cancer. 17 (2017) 130, https://doi.org/10.1186/s12885-017-3116-9.
[8] S.T. Arthur, B.A. Van Doren, D. Roy, J.M. Noone, E. Zacherle, C.M. Blanchette, Cachexia among US cancer patients, J. Med. Econ. 19 (2016) 874–880, https://doi.org/10.1080/13696998.2016.1181640.
[9] P. Liu, Q. Hao, S. Hai, H. Wang, L. Cao, B. Dong, Sarcopenia as a predictor of all-cause mortality among community-dwelling older people: a systematic review and meta-analysis, Maturitas. 103 (2017) 16–22, https://doi.org/10.1016/j.maturitas.2017.04.007.
[10] M.-L.-N. McDonald, E.F.M. Wouters, E. Rutten, R. Casaburi, S.I. Rennard, D. A. Lomas, M. Bamman, B. Celli, A. Agusti, R. Tal-Singer, C.P. Hersh, M. Dransfield, E.K. Silverman, It's more than low BMI: prevalence of cachexia and associated mortality in COPD, Respir. Res. 20 (2019) 100, https://doi.org/10.1186/s12931-019-1073-3.
[11] E.J. Roeland, K. Bohlke, V.E. Baracos, E. Bruera, E. Del Fabbro, S. Dixon, M. Fallon, J. Herrstedt, H. Lau, M. Platek, H.S. Rugo, H.H. Schnipper, T.J. Smith, W. Tan, C.L. Loprinzi, Management of cancer cachexia: ASCO guideline, J. Clin. Oncol. Off. J. Am. Soc. Clin. Oncol. 38 (2020) 2438–2453, https://doi.org/10.1200/JCO.20.00611.
[12] J. Arends, F. Strasser, S. Gonella, T.S. Solheim, C. Madeddu, P. Ravasco, L. Buonaccorso, M.A.E. de van der Schueren, C. Baldwin, M. Chasen, C.I. Ripamonti, Cancer cachexia in adult patients: ESMO Clinical Practice Guidelines(☆)., ESMO Open. 6 (2021) 100092.
[13] C. Beaudart, E. McCloskey, O. Bruyère, M. Cesari, Y. Rolland, R. Rizzoli, I. Araujo de Carvalho, J. Amuthavalli Thiyagarajan, I. Bautmans, M.-C. Bertière, M. L. Brandi, N.M. Al-Daghri, N. Burlet, E. Cavalier, F. Cerreta, A. Cherubini, R. Fielding, E. Gielen, F. Landi, J. Petermans, J.-Y. Reginster, M. Visser, J. Kanis, C. Cooper, Sarcopenia in daily practice: assessment and management, BMC Geriatr. 16 (2016) 170, https://doi.org/10.1186/s12877-016-0349-4.
[14] M.Ø. Fosbøl, B. Zerahn, Contemporary methods of body composition measurement, Clin. Physiol. Funct. Imaging. 35 (2015) 81–97, https://doi.org/10.1111/cpf.12152.
[15] D. Albano, C. Messina, J. Vitale, L.M. Sconfienza, Imaging of sarcopenia: old evidence and new insights, Eur. Radiol. 30 (2020) 2199–2208, https://doi.org/10.1007/s00330-019-06573-2.
[16] C.M.M. Prado, L.A. Birdsell, V.E. Baracos, The emerging role of computerized tomography in assessing cancer cachexia, Curr. Opin. Support. Palliat. Care. 3 (2009) 269–275, https://doi.org/10.1097/SPC.0b013e328331124a.
[17] X. Zhang, X. Xie, Q. Dou, C. Liu, W. Zhang, Y. Yang, R. Deng, A.S.K. Cheng, Association of sarcopenic obesity with the risk of all-cause mortality among adults over a broad range of different settings: a updated meta-analysis, BMC Geriatr. 19 (2019) 183, https://doi.org/10.1186/s12877-019-1195-y.
[18] C.B. Monti, M. Codari, C.N. De Cecco, F. Secchi, F. Sardanelli, A.E. Stillman, Novel imaging biomarkers: epicardial adipose tissue evaluation, Br. J. Radiol. 93 (2020) 20190770, https://doi.org/10.1259/bjr.20190770.
[19] J.A. Brink, J.P. Heiken, G. Wang, K.W. McEnery, F.J. Schlueter, M.W. Vannier, Helical CT: principles and technical considerations., Radiogr. a Rev. Publ. Radiol. Soc. North Am. Inc. 14 (1994) 887–893. https://doi.org/10.1148/radiographics.14.4.7938775.
[20] D. Sottier, J.-M. Petit, S. Guiu, S. Hamza, H. Benhamiche, P. Hillon, J.-P. Cercueil, D. Krausé, B. Guiu, Quantification of the visceral and subcutaneous fat by computed tomography: interobserver correlation of a single slice technique, Diagn. Interv. Imaging. 94 (2013) 879–884, https://doi.org/10.1016/j.diii.2013.04.006.
[21] L.W. Goldman, Principles of CT: multislice CT, J. Nucl. Med. Technol. 36 (2008) 56–57, https://doi.org/10.2967/jnmt.107.044826.
[22] M. Prokop, Multislice CT: technical principles and future trends, Eur. Radiol. 13 (Suppl 5) (2003) M3–13, https://doi.org/10.1007/s00330-003-2178-z.
[23] T.R.C. Johnson, Dual-energy CT: general principles, AJR. Am. J. Roentgenol. 199 (2012) S3–8, https://doi.org/10.2214/AJR.12.9116.
[24] P.S. Sanghavi, B.G. Jankharia, Applications of dual energy CT in clinical practice: A pictorial essay, Indian J. Radiol. Imaging. 29 (2019) 289–298, https://doi.org/10.4103/ijri.IJRI_241_19.
[25] M. Saito, S. Sagara, A simple formulation for deriving effective atomic numbers via electron density calibration from dual-energy CT data in the human body, Med. Phys. 44 (2017) 2293–2303, https://doi.org/10.1002/mp.12176.
[26] D. Marin, D.T. Boll, A. Mileto, R.C. Nelson, State of the art: dual-energy CT of the abdomen, Radiology. 271 (2014) 327–342, https://doi.org/10.1148/radiol.14131480.
[27] A. Gücük, U. Uyetürk, Usefulness of hounsfield unit and density in the assessment and treatment of urinary stones, World J. Nephrol. 3 (2014) 282–286, https://doi.org/10.5527/wjn.v3.i4.282.
[28] K.J. Rosenquist, A. Pedley, J.M. Massaro, K.E. Therkelsen, J.M. Murabito, U. Hoffmann, C.S. Fox, Visceral and subcutaneous fat quality and cardiometabolic risk, JACC. Cardiovasc. Imaging. 6 (2013) 762–771, https://doi.org/10.1016/j.jcmg.2012.11.021.
[29] G.D. Ceniccola, M.G. Castro, S.M.F. Piovacari, L.M. Horie, F.G. Corrêa, A.P. N. Barrere, D.O. Toledo, Current technologies in body composition assessment: advantages and disadvantages, Nutrition. 62 (2019) 25–31, https://doi.org/10.1016/j.nut.2018.11.028.
[30] M.S. Mundi, J.J. Patel, R. Martindale, Body Composition Technology: Implications for the ICU, Nutr. Clin. Pract. Off. Publ. Am. Soc. Parenter. Enter. Nutr. 34 (2019) 48–58, https://doi.org/10.1002/ncp.10230.
[31] L.M. Teigen, A.J. Kuchnia, M. Mourtzakis, C.P. Earthman, The use of technology for estimating body composition (strengths and weaknesses of common modalities in a clinical setting [formula: see text]), Nutr. Clin. Pract. Off. Publ. Am. Soc. Parenter. Enter. Nutr. 32 (2017) 20–29, https://doi.org/10.1177/0884533616676264.
[32] D. Bolus, D. Morgan, L. Berland, Effective use of the Hounsfield unit in the age of variable energy CT, Abdom. Radiol. (New York) 42 (2017) 766–771, https://doi.org/10.1007/s00261-017-1052-4.
[33] B.C. Stoel, J. Stolk, Optimization and standardization of lung densitometry in the assessment of pulmonary emphysema, Invest. Radiol. 39 (2004) 681–688, https://doi.org/10.1097/00004424-200411000-00006.
[34] P. Boris, F. Bundgaard, A. Olsen, The CT (Hounsfield unit) number of brain tissue in healthy infants. A new reliable method for detection of possible degenerative disease, Child's Nerv. Syst. ChNS Off. J. Int. Soc Pediatr. Neurosurg. 3 (1987) 175–177, https://doi.org/10.1007/BF00717896.
[35] D.L. Duren, R.J. Sherwood, S.A. Czerwinski, M. Lee, A.C. Choh, R.M. Siervogel, W. Cameron Chumlea, Body composition methods: comparisons and interpretation, J. Diabetes Sci. Technol. 2 (2008) 1139–1146, https://doi.org/10.1177/193229680800200623.

[36] Y.-C. Peng, C.-H. Wu, Y.-W. Tien, T.-P. Lu, Y.-H. Wang, B.-B. Chen, Preoperative sarcopenia is associated with poor overall survival in pancreatic cancer patients following pancreaticoduodenectomy, Eur. Radiol. 31 (2021) 2472–2481, https://doi.org/10.1007/s00330-020-07294-7.

[37] C. Yip, V. Goh, A. Davies, J. Gossage, R. Mitchell-Hay, O. Hynes, N. Maisey, P. Ross, A. Gaya, D.B. Landau, G.J. Cook, N. Griffin, R. Mason, Assessment of sarcopenia and changes in body composition after neoadjuvant chemotherapy and associations with clinical outcomes in oesophageal cancer, Eur. Radiol. 24 (2014) 998–1005, https://doi.org/10.1007/s00330-014-3110-4.

[38] M. Borga, J. West, J.D. Bell, N.C. Harvey, T. Romu, S.B. Heymsfield, O. Dahlqvist Leinhard, Advanced body composition assessment: from body mass index to body composition profiling, J. Investig. Med. Off. Publ. Am. Fed. Clin. Res. 66 (2018) 1–9, https://doi.org/10.1136/jim-2018-000722.

[39] N. Mitsiopoulos, R.N. Baumgartner, S.B. Heymsfield, W. Lyons, D. Gallagher, R. Ross, Cadaver validation of skeletal muscle measurement by magnetic resonance imaging and computerized tomography, J. Appl. Physiol. 85 (1998) 115–122, https://doi.org/10.1152/jappl.1998.85.1.115.

[40] F.-Z. Wang, H. Sun, J. Zhou, L.-L. Sun, S.-N. Pan, Reliability and validity of abdominal skeletal muscle area measurement using magnetic resonance imaging, Acad. Radiol. (2020), https://doi.org/10.1016/j.acra.2020.09.013.

[41] A. Faron, A.M. Sprinkart, D.L.R. Kuetting, A. Feisst, A. Isaak, C. Endler, J. Chang, S. Nowak, W. Block, D. Thomas, U. Attenberger, J.A. Luetkens, Body composition analysis using CT and MRI: intra-individual intermodal comparison of muscle mass and myosteatosis, Sci. Rep. 10 (2020) 11765, https://doi.org/10.1038/s41598-020-68797-3.

[42] L. Schweitzer, C. Geisler, M. Pourhassan, W. Braun, C.-C. Glüer, A. Bosy-Westphal, M.J. Müller, Estimation of skeletal muscle mass and visceral adipose tissue volume by a single magnetic resonance imaging slice in healthy elderly adults, J. Nutr. 146 (2016) 2143–2148, https://doi.org/10.3945/jn.116.236844.

[43] W. Shen, M. Punyanitya, Z. Wang, D. Gallagher, M.-P. St-Onge, J. Albu, S. B. Heymsfield, S. Heshka, Total body skeletal muscle and adipose tissue volumes: estimation from a single abdominal cross-sectional image, J. Appl. Physiol. 97 (2004) 2333–2338, https://doi.org/10.1152/japplphysiol.00744.2004.

[44] B. Amini, S.P. Boyle, R.D. Boutin, L. Lenchik, Approaches to assessment of muscle mass and myosteatosis on computed tomography: a systematic review, J. Gerontol. A. Biol. Sci. Med. Sci. 74 (2019) 1671–1678, https://doi.org/10.1093/gerona/glz034.

[45] I. Almada-Correia, P.M. Neves, A. Mäkitie, P. Ravasco, Body composition evaluation in head and neck cancer patients: a review, Front. Oncol. 9 (2019) 1112, https://doi.org/10.3389/fonc.2019.01112.

[46] R. Matsuyama, K. Maeda, Y. Yamanaka, Y. Ishida, R. Kato, T. Nonogaki, A. Shimizu, J. Ueshima, Y. Kazaoka, T. Hayashi, K. Ito, A. Furuhashi, T. Ono, N. Mori, Assessing skeletal muscle mass based on the cross-sectional area of muscles at the 12th thoracic vertebra level on computed tomography in patients with oral squamous cell carcinoma, Oral Oncol. 113 (2021), 105126, https://doi.org/10.1016/j.oraloncology.2020.105126.

[47] M.A. Waduud, P. Adusumilli, M. Drozd, M.A. Bailey, G. Cuthbert, C. Hammond, J. A. Scott, Volumetric versus single slice measurements of core abdominal muscle for sarcopenia, Br. J. Radiol. 92 (2019) 20180434, https://doi.org/10.1259/bjr.20180434.

[48] A. Faron, J.A. Luetkens, F.C. Schmeel, D.L.R. Kuetting, D. Thomas, A. M. Sprinkart, Quantification of fat and skeletal muscle tissue at abdominal computed tomography: associations between single-slice measurements and total compartment volumes, Abdom. Radiol. (New York) 44 (2019) 1907–1916, https://doi.org/10.1007/s00261-019-01912-9.

[49] B.A. Derstine, S.A. Holcombe, B.E. Ross, N.C. Wang, G.L. Su, S.C. Wang, Skeletal muscle cutoff values for sarcopenia diagnosis using T10 to L5 measurements in a healthy US population, Sci. Rep. 8 (2018) 11369, https://doi.org/10.1038/s41598-018-29825-5.

[50] T. Irlbeck, J.M. Massaro, F. Bamberg, C.J. O'Donnell, U. Hoffmann, C.S. Fox, Association between single-slice measurements of visceral and abdominal subcutaneous adipose tissue with volumetric measurements: the Framingham Heart Study, Int. J. Obes. (Lond) 34 (2010) 781–787, https://doi.org/10.1038/ijo.2009.279.

[51] L.E. Daly, C.M. Prado, A.M. Ryan, A window beneath the skin: how computed tomography assessment of body composition can assist in the identification of hidden wasting conditions in oncology that profoundly impact outcomes, Proc. Nutr. Soc. 77 (2018) 135–151, https://doi.org/10.1017/S0029665118000046.

[52] S.L. Doyle, A.M. Bennett, C.L. Donohoe, A.M. Mongan, J.M. Howard, F. E. Lithander, G.P. Pidgeon, J.V. Reynolds, J. Lysaght, Establishing computed tomography-defined visceral fat area thresholds for use in obesity-related cancer research, Nutr. Res. 33 (2013) 171–179, https://doi.org/10.1016/j.nutres.2012.12.007.

[53] S. Yoo, M.-W. Sung, H. Kim, CT-defined visceral adipose tissue thresholds for identifying metabolic complications: a cross-sectional study in the United Arab Emirates, BMJ Open. 10 (2020), e031181, https://doi.org/10.1136/bmjopen-2019-031181.

[54] J. Xiao, V.C. Mazurak, T.A. Olobatuyi, B.J. Caan, C.M. Prado, Visceral adiposity and cancer survival: a review of imaging studies, Eur. J. Cancer Care (Engl). 27 (2018), e12611, https://doi.org/10.1111/ecc.12611.

[55] 3D Slicer, online availabe: https://www.slicer.org/. Accessed on 19/07/2021.

[56] Medical Imaging Interaction Toolkit (MITK), online available: https://docs.mitk.org/nightly/index.html. Accessed on 19/07/2021.

[57] ITK Snap, online available: http://www.itksnap.org/pmwiki/pmwiki.php. Accessed on 19/07/2021.

[58] ePAD imaging platform, online available: https://epad.stanford.edu/. Accessed on 19/07/2021.

[59] ImageJ, online available: https://imagej.nih.gov/ij/download.html. Accessed on 19/07/2021.

[60] W. Chen, R. Smith, S.-Y. Ji, K.R. Ward, K. Najarian, Automated ventricular systems segmentation in brain CT images by combining low-level segmentation and high-level template matching, BMC Med. Inform. Decis. Mak. 9 (2009) S4, https://doi.org/10.1186/1472-6947-9-S1-S4.

[61] S. Minaee, Y.Y. Boykov, F. Porikli, A.J. Plaza, N. Kehtarnavaz, D. Terzopoulos, Image segmentation using deep learning: a survey, IEEE Trans. Pattern Anal. Mach. Intell. (2021), https://doi.org/10.1109/TPAMI.2021.3059968.

[62] SOPHiA Genetics, The SOPHiA DDMTM platform, online available: https://www.sophiagenetics.com/technology. Accessed on 19/07/2021.

[63] Y. Tong, J.K. Udupa, D.A. Torigian, Optimization of abdominal fat quantification on CT imaging through use of standardized anatomic space: a novel approach, Med. Phys. 41 (2014) 63501, https://doi.org/10.1118/1.4876275.

[64] I. Ozola-Zālīte, E.B. Mark, T. Gudauskas, V. Lyadov, S.S. Olesen, A.M. Drewes, A. Pukitis, J.B. Frokjær, Reliability and validity of the new VikingSlice software for computed tomography body composition analysis, Eur. J. Clin. Nutr. 73 (2019) 54–61, https://doi.org/10.1038/s41430-018-0110-5.

[65] Osirix DICOM Viewer, online available: https://www.osirix-viewer.com/. Accessed on 19/07/2021.

[66] SliceOmatic, online available: https://www.tomovision.com/products/sliceomatic.html. Accessed on 19/07/2021.

[67] S.D. Mensink, J.W. Spliethoff, R. Belder, J.M. Klaase, R. Bezooijen, C.H. Slump, Development of automated quantification of visceral and subcutaneous adipose tissue volumes from abdominal CT scans, 7963 (2011) 79632Q-79632Q–12. https://doi.org/10.1117/12.878017.

[68] S. Ontiveros, J.A. Yagüe, R. Jiménez, F. Brosed, Computer tomography 3D edge detection comparative for metrology applications, Procedia Eng. 63 (2013) 710–719, https://doi.org/10.1016/j.proeng.2013.08.263.

[69] P. Hu, Y. Huo, D. Kong, J.J. Carr, R.G. Abramson, K.G. Hartley, B.A. Landman, Automated Characterization of Body Composition and Frailty with Clinically Acquired CT., Comput. Methods Clin. Appl. Musculoskelet. Imaging 5th Int. Work. MSKI 2017, Held Conjunction with MICCAI 2017, Quebec City, QC, Canada, Sept. 10, 2017, Revis. Sel. Pap. MSKI (Worksh... 10734 (2018) 25–35.

[70] P. Decazes, A. Rouquette, A. Chetrit, P. Vera, I. Gardin, Automatic measurement of the total visceral adipose tissue from computed tomography images by using a multi-atlas segmentation method, J. Comput. Assist. Tomogr. 42 (2018) 139–145, https://doi.org/10.1097/RCT.0000000000000652.

[71] R. Hemke, C.G. Buckless, A. Tsao, B. Wang, M. Torriani, Deep learning for automated segmentation of pelvic muscles, fat, and bone from CT studies for body composition assessment, Skeletal Radiol. 49 (2020) 387–395, https://doi.org/10.1007/s00256-019-03289-8.

[72] M.T. Paris, P. Tandon, D.K. Heyland, H. Furberg, T. Premji, G. Low, M. Mourtzakis, Automated body composition analysis of clinically acquired computed tomography scans using neural networks, Clin. Nutr. 39 (2020) 3049–3055, https://doi.org/10.1016/j.clnu.2020.01.008.

[73] S. Koitka, L. Kroll, E. Malamutmann, A. Oezcelik, F. Nensa, Fully automated body composition analysis in routine CT imaging using 3D semantic segmentation convolutional neural networks, Eur. Radiol. 31 (2021) 1795–1804, https://doi.org/10.1007/s00330-020-07147-3.

[74] S. Dabiri, K. Popuri, E.M. Cespedes Feliciano, B.J. Caan, V.E. Baracos, M.F. Beg, Muscle segmentation in axial computed tomography (CT) images at the lumbar (L3) and thoracic (T4) levels for body composition analysis, Comput. Med. Imaging Graph. Off. J. Comput. Med. Imaging Soc. 75 (2019) 47–55, https://doi.org/10.1016/j.compmedimag.2019.04.007.

[75] Y. Wang, T. Thai, K. Moore, K. Ding, S. McMeekin, H. Liu, B. Zheng, Quantitative measurement of adiposity using CT images to predict the benefit of bevacizumab-based chemotherapy in epithelial ovarian cancer patients, Oncol. Lett. 12 (2016) 680–686, https://doi.org/10.3892/ol.2016.4648.

[76] J. Kullberg, A. Hedström, J. Brandberg, R. Strand, L. Johansson, G. Bergström, H. Ahlström, Automated analysis of liver fat, muscle and adipose tissue distribution from CT suitable for large-scale studies, Sci. Rep. 7 (2017) 10425, https://doi.org/10.1038/s41598-017-08925-8.

[77] L.L.G.C. Ackermans, L. Volmer, L. Wee, R. Brecheisen, P. Sánchez-González, A. P. Seiffert, E.J. Gómez, A. Dekker, J.A. Ten Bosch, S.M.W. Olde Damink, T. J. Blokhuis, Deep learning automated segmentation for muscle and adipose tissue from abdominal computed tomography in polytrauma patients, Sensors (Basel) 21 (2021) 2083, https://doi.org/10.3390/s21062083.

[78] DICOM Grid, inc. AMBRA, online available: https://ambrahealth.com/. Accessed on 19/07/2021.

[79] RADSOURCE LLC, ProtonPACS, online available: https://radsource.us/protonpacs-pacs/. Accessed on 19/07/2021.

[80] E. Deluche, S. Leobon, J.C. Desport, L. Venat-Bouvet, J. Usseglio, N. Tubiana-Mathieu, Impact of body composition on outcome in patients with early breast cancer, Support. Care Cancer Off. J. Multinatl. Assoc. Support. Care Cancer. 26 (2018) 861–868, https://doi.org/10.1007/s00520-017-3902-6.

[81] T. Iwase, T. Sangai, T. Nagashima, M. Sakakibara, J. Sakakibara, S. Hayama, E. Ishigami, T. Masuda, M. Miyazaki, Impact of body fat distribution on neoadjuvant chemotherapy outcomes in advanced breast cancer patients, Cancer Med. 5 (2016) 41–48, https://doi.org/10.1002/cam4.571.

[82] G.F.P. Aleixo, G.R. Williams, K.A. Nyrop, H.B. Muss, S.S. Shachar, Muscle composition and outcomes in patients with breast cancer: meta-analysis and systematic review, Breast Cancer Res. Treat. 177 (2019) 569–579, https://doi.org/10.1007/s10549-019-05352-3.

[83] S.J. Cushen, D.G. Power, K.P. Murphy, R. McDermott, B.T. Griffin, M. Lim, L. Daly, P. MacEneaney, K. O'Sullivan, C.M. Prado, A.M. Ryan, Impact of body composition parameters on clinical outcomes in patients with metastatic castrate-resistant prostate cancer treated with docetaxel, Clin. Nutr. ESPEN. 13 (2016) e39–e45, https://doi.org/10.1016/j.clnesp.2016.04.001.
[84] R.B. den Boer, K.I. Jones, S. Ash, G.I. van Boxel, R.S. Gillies, T. O'Donnell, J. P. Ruurda, B. Sgromo, M.A. Silva, N.D. Maynard, Impact on postoperative complications of changes in skeletal muscle mass during neoadjuvant chemotherapy for gastro-oesophageal cancer, BJS Open. 4 (2020) 847–854, https://doi.org/10.1002/bjs5.50331.
[85] H. Su, J. Ruan, T. Chen, E. Lin, L. Shi, CT-assessed sarcopenia is a predictive factor for both long-term and short-term outcomes in gastrointestinal oncology patients: a systematic review and meta-analysis., Cancer Imaging Off, Publ. Int. Cancer Imaging Soc. 19 (2019) 82, https://doi.org/10.1186/s40644-019-0270-0.
[86] J.A. Elliott, S.L. Doyle, C.F. Murphy, S. King, E.M. Guinan, P. Beddy, N. Ravi, J. V. Reynolds, Sarcopenia: prevalence, and impact on operative and oncologic outcomes in the multimodal management of locally advanced esophageal cancer, Ann. Surg. 266 (2017) 822–830, https://doi.org/10.1097/SLA.0000000000002398.
[87] D. Tamandl, M. Paireder, R. Asari, P.A. Baltzer, S.F. Schoppmann, A. Ba-Ssalamah, Markers of sarcopenia quantified by computed tomography predict adverse long-term outcome in patients with resected oesophageal or gastro-oesophageal junction cancer, Eur. Radiol. 26 (2016) 1359–1367, https://doi.org/10.1007/s00330-015-3963-1.
[88] S.K. Kamarajah, J. Bundred, B.H.L. Tan, Body composition assessment and sarcopenia in patients with gastric cancer: a systematic review and meta-analysis, Gastric Cancer Off J. Int. Gastric Cancer Assoc. Japanese Gastric Cancer Assoc. 22 (2019) 10–22, https://doi.org/10.1007/s10120-018-0882-2.
[89] D. Basile, A. Parnofiello, M.G. Vitale, F. Cortiula, L. Gerratana, V. Fanotto, C. Lisanti, G. Pelizzari, E. Ongaro, M. Bartoletti, S.K. Garattini, V.J. Andreotti, A. Bacco, D. Iacono, M. Bonotto, M. Casagrande, P. Ermacora, F. Puglisi, N. Pella, G. Fasola, G. Aprile, G.G. Cardellino, The IMPACT study: early loss of skeletal muscle mass in advanced pancreatic cancer patients, J. Cachexia. Sarcopenia Muscle. 10 (2019) 368–377, https://doi.org/10.1002/jcsm.12368.
[90] D. Black, C. Mackay, G. Ramsay, Z. Hamoodi, S. Nanthakumaran, K.G.M. Park, M. A. Loudon, C.H. Richards, Prognostic value of computed tomography: measured parameters of body composition in primary operable gastrointestinal cancers, Ann. Surg. Oncol. 24 (2017) 2241–2251, https://doi.org/10.1245/s10434-017-5829-z.
[91] H. Fukushima, Y. Nakanishi, M. Kataoka, K. Tobisu, F. Koga, Prognostic significance of sarcopenia in patients with metastatic renal cell carcinoma, J. Urol. 195 (2016) 26–32, https://doi.org/10.1016/j.juro.2015.08.071.
[92] J.H.R.J. Degens, K.J.C. Sanders, E.E.C. de Jong, H.J.M. Groen, E.F. Smit, J. G. Aerts, A.M.W.J. Schols, A.-M.C. Dingemans, The prognostic value of early onset, CT derived loss of muscle and adipose tissue during chemotherapy in metastatic non-small cell lung cancer, Lung Cancer. 133 (2019) 130–135, https://doi.org/10.1016/j.lungcan.2019.05.021.
[93] L.E. Daly, É.B. Ní Bhuachalla, D.G. Power, S.J. Cushen, K. James, A.M. Ryan, Loss of skeletal muscle during systemic chemotherapy is prognostic of poor survival in patients with foregut cancer, J. Cachexia. Sarcopenia Muscle. 9 (2018) 315–325, https://doi.org/10.1002/jcsm.12267.
[94] K. Sugiyama, Y. Narita, S. Mitani, K. Honda, T. Masuishi, H. Taniguchi, S. Kadowaki, T. Ura, M. Ando, M. Tajika, K. Muro, Baseline Sarcopenia and Skeletal Muscle Loss During Chemotherapy Affect Survival Outcomes in Metastatic Gastric Cancer., Anticancer Res. 38 (2018) 5859–5866. https://doi.org/10.21873/anticanres.12928.
[95] I.J.G. Rutten, D.P.J. van Dijk, R.F.P.M. Kruitwagen, R.G.H. Beets-Tan, S.W. M. Olde Damink, T. van Gorp, Loss of skeletal muscle during neoadjuvant chemotherapy is related to decreased survival in ovarian cancer patients, J. Cachexia. Sarcopenia Muscle. 7 (2016) 458–466, https://doi.org/10.1002/jcsm.12107.
[96] F. Mazzuca, C.E. Onesti, M. Roberto, M. Di Girolamo, A. Botticelli, P. Begini, L. Strigari, P. Marchetti, M. Muscaritoli, Lean body mass wasting and toxicity in early breast cancer patients receiving anthracyclines., Oncotarget. 9 (2018) 25714–25722. https://doi.org/10.18632/oncotarget.25394.
[97] A.W. Wendrich, J.E. Swartz, S.I. Bril, I. Wegner, A. de Graeff, E.J. Smid, R. de Bree, A.J. Pothen, Low skeletal muscle mass is a predictive factor for chemotherapy dose-limiting toxicity in patients with locally advanced head and neck cancer, Oral Oncol. 71 (2017) 26–33, https://doi.org/10.1016/j.oraloncology.2017.05.012.
[98] M.I. van Rijn-Dekker, L. van den Bosch, J.G.M. van den Hoek, H.P. Bijl, E.S. M. van Aken, A. van der Hoorn, S.F. Oosting, G.B. Halmos, M.J.H. Witjes, H. P. van der Laan, J.A. Langendijk, R.J.H.M. Steenbakkers, Impact of sarcopenia on survival and late toxicity in head and neck cancer patients treated with radiotherapy, Radiother. Oncol. J. Eur. Soc. Ther. Radiol. Oncol. 147 (2020) 103–110, https://doi.org/10.1016/j.radonc.2020.03.014.
[99] S.A. Staley, K. Tucker, M. Newton, M. Ertel, J. Oldan, I. Doherty, L. West, Y. Zhang, P.A. Gehrig, Sarcopenia as a predictor of survival and chemotoxicity in patients with epithelial ovarian cancer receiving platinum and taxane-based chemotherapy, Gynecol. Oncol. 156 (2020) 695–700, https://doi.org/10.1016/j.ygyno.2020.01.003.
[100] S.S. Shachar, A.M. Deal, M. Weinberg, K.A. Nyrop, G.R. Williams, T.F. Nishijima, J.M. Benbow, H.B. Muss, Skeletal muscle measures as predictors of toxicity, hospitalization, and survival in patients with metastatic breast cancer receiving taxane-based chemotherapy, Clin. Cancer Res. an Off. J. Am. Assoc. Cancer Res. 23 (2017) 658–665, https://doi.org/10.1158/1078-0432.CCR-16-0940.
[101] B.H.L. Tan, K. Brammer, N. Randhawa, N.T. Welch, S.L. Parsons, E.J. James, J. A. Catton, Sarcopenia is associated with toxicity in patients undergoing neo-adjuvant chemotherapy for oesophago-gastric cancer, Eur. J. Surg. Oncol. J. Eur. Soc. Surg. Oncol. Br. Assoc. Surg. Oncol. 41 (2015) 333–338, https://doi.org/10.1016/j.ejso.2014.11.040.
[102] E.H. van Roekel, M.J.L. Bours, M.E.M. Te Molder, J.J.L. Breedveld-Peters, S.W. M. Olde Damink, L.J. Schouten, S. Sanduleanu, G.L. Beets, M.P. Weijenberg, Associations of adipose and muscle tissue parameters at colorectal cancer diagnosis with long-term health-related quality of life, Qual. Life Res. an Int. J. Qual. Life Asp. Treat. Care Rehabil. 26 (2017) 1745–1759, https://doi.org/10.1007/s11136-017-1539-z.
[103] B. Gigic, J. Nattenmüller, M. Schneider, Y. Kulu, K.L. Syrjala, J. Böhm, P. Schrotz-King, H. Brenner, G.A. Colditz, J.C. Figueiredo, W.M. Grady, C.I. Li, D. Shibata, E. M. Siegel, A.T. Toriola, H.-U. Kauczor, A. Ulrich, C.M. Ulrich, The role of CT-quantified body composition on longitudinal health-related quality of life in colorectal cancer patients: the colocare study, Nutrients. 12 (2020) 1247, https://doi.org/10.3390/nu12051247.
[104] P.R. Joyce, R. O'Dempsey, G. Kirby, C. Anstey, A retrospective observational study of sarcopenia and outcomes in critically ill patients, Anaesth. Intensive Care. 48 (2020) 229–235, https://doi.org/10.1177/0310057X20922234.
[105] S.H. Loosen, M. Schulze-Hagen, T. Püngel, L. Bündgens, T. Wirtz, J.N. Kather, M. Vucur, P. Paffenholz, M. Demir, P. Bruners, C. Kuhl, C. Trautwein, F. Tacke, T. Luedde, A. Koch, C. Roderburg, Skeletal muscle composition predicts outcome in critically Ill patients, Crit. Care Explor. 2 (2020), e0171, https://doi.org/10.1097/CCE.0000000000000171.
[106] D.O. Toledo, A.M. Carvalho, A.M.R.R. Oliveira, J.M. Toloi, A.C. Silva, J. Francisco de Mattos Farah, C.M. Prado, J.M.J. Silva, The use of computed tomography images as a prognostic marker in critically ill cancer patients, Clin. Nutr. ESPEN. 25 (2018) 114–120, https://doi.org/10.1016/j.clnesp.2018.03.122.
[107] P.A. de Hoogt, K.W. Reisinger, J.J.W. Tegels, J.W.A.M. Bosmans, F. Tijssen, J.H. M.B. Stoot, Functional compromise cohort study (FCCS): sarcopenia is a strong predictor of mortality in the intensive care unit, World J. Surg. 42 (2018) 1733–1741, https://doi.org/10.1007/s00268-017-4386-8.
[108] M.M. Dusseaux, S. Antoun, S. Grigioni, G. Béduneau, D. Carpentier, C. Girault, S. Grange, F. Tamion, Skeletal muscle mass and adipose tissue alteration in critically ill patients, PLoS One. 14 (2019), e0216991, https://doi.org/10.1371/journal.pone.0216991.
[109] D.M. Zumsteg, C.E. Chu, M.J. Midwinter, Radiographic assessment of sarcopenia in the trauma setting: a systematic review, e000414 e000414, Trauma Surg. Acute Care Open. 5 (2020), https://doi.org/10.1136/tsaco-2019-000414.
[110] M.E. Deren, J. Babu, E.M. Cohen, J. Machan, C.T. Born, R. Hayda, Increased mortality in elderly patients with sarcopenia and acetabular fractures, J. Bone Joint Surg. Am. 99 (2017) 200–206, https://doi.org/10.2106/JBJS.16.00734.
[111] P.M. Mitchell, C.A. Collinge, D.E. O'Neill, J.E. Bible, H.R. Mir, Sarcopenia is predictive of 1-year mortality after acetabular fractures in elderly patients, J. Orthop. Trauma. 32 (2018) 278–282, https://doi.org/10.1097/BOT.0000000000001159.
[112] C.-D. Chang, J.S. Wu, J.N. Mhuircheartaigh, M.G. Hochman, E.K. Rodriguez, P. T. Appleton, C.J. Mcmahon, Effect of sarcopenia on clinical and surgical outcome in elderly patients with proximal femur fractures, Skeletal Radiol. 47 (2018) 771–777, https://doi.org/10.1007/s00256-017-2848-6.
[113] S.-E. Byun, S. Kim, K.-H. Kim, Y.-C. Ha, Psoas cross-sectional area as a predictor of mortality and a diagnostic tool for sarcopenia in hip fracture patients, J. Bone Miner. Metab. 37 (2019) 871–879, https://doi.org/10.1007/s00774-019-00986-1.
[114] R.D. Boutin, S. Bamrungchart, C.P. Bateni, D.P. Beavers, K.M. Beavers, J. P. Meehan, L. Lenchik, CT of patients with hip fracture: muscle size and attenuation help predict mortality, AJR. Am. J. Roentgenol. 208 (2017) W208–W215, https://doi.org/10.2214/AJR.16.17226.
[115] J. Trotter, J. Johnston, A. Ng, M. Gatt, J. MacFie, C. McNaught, Is sarcopenia a useful predictor of outcome in patients after emergency laparotomy? A study using the NELA database, Ann. R. Coll. Surg. Engl. 100 (2018) 377–381, https://doi.org/10.1308/rcsann.2017.0230.
[116] G. Simpson, N. Manu, C. Magee, J. Wilson, S. Moug, D. Vimalachandran, Measuring sarcopenia on pre-operative CT in older adults undergoing emergency laparotomy: a comparison of three different calculations, Int. J. Colorectal Dis. 35 (2020) 1095–1102, https://doi.org/10.1007/s00384-020-03570-6.
[117] C. McQuade, D.O. Kavanagh, C. O'Brien, K. Hunter, D. Nally, C. Hickie, E. Ward, W.C. Torreggiani, CT-determined sarcopenia as a predictor of post-operative outcomes in patients undergoing an emergency laparotomy, Clin. Imaging. 79 (2021) 273–277, https://doi.org/10.1016/j.clinimag.2021.05.015.
[118] E. Brandt, L.T. Tengberg, M. Bay-Nielsen, Sarcopenia predicts 90-day mortality in elderly patients undergoing emergency abdominal surgery, Abdom. Radiol. (New York) 44 (2019) 1155–1160, https://doi.org/10.1007/s00261-018-1870-z.
[119] H. Okamura, N. Kimura, M. Mieno, K. Yuri, A. Yamaguchi, Preoperative sarcopenia is associated with late mortality after off-pump coronary artery bypass grafting, Eur. J. Cardio-Thoracic Surg. Off. J. Eur. Assoc. Cardio-Thoracic Surg. 58 (2020) 121–129, https://doi.org/10.1093/ejcts/ezz378.
[120] S.L. Olson, A.M. Panthofer, D.J. Harris, W.D.J. Jordan, M.A. Farber, R.P. Cambria, J.S. Matsumura, CT-derived pretreatment thoracic sarcopenia is associated with late mortality after thoracic endovascular aortic repair, Ann. Vasc. Surg. 66 (2020) 171–178, https://doi.org/10.1016/j.avsg.2019.10.089.
[121] J. Zuckerman, M. Ades, L. Mullie, A. Trnkus, J.-F. Morin, Y. Langlois, F. Ma, M. Levental, J.A. Morais, J. Afilalo, Psoas muscle area and length of stay in older adults undergoing cardiac operations, Ann. Thorac. Surg. 103 (2017) 1498–1504, https://doi.org/10.1016/j.athoracsur.2016.09.005.

[122] U. Nemec, B. Heidinger, C. Sokas, L. Chu, R.L. Eisenberg, Diagnosing sarcopenia on thoracic computed tomography: quantitative assessment of skeletal muscle mass in patients undergoing transcatheter aortic valve replacement, Acad. Radiol. 24 (2017) 1154–1161, https://doi.org/10.1016/j.acra.2017.02.008.
[123] S. Schiaffino, D. Albano, A. Cozzi, C. Messina, R. Arioli, C. Bnà, A. Bruno, L. A. Carbonaro, A. Carriero, S. Carriero, P.S.C. Danna, E. D'Ascoli, C. De Berardinis, G. Della Pepa, Z. Falaschi, S. Gitto, A.E. Malavazos, G. Mauri, L. Monfardini, A. Paschè, R. Rizzati, F. Secchi, A. Vanzulli, V. Tombini, I. Vicentin, D. Zagaria, F. Sardanelli, L.M. Sconfienza, CT-derived chest muscle metrics for outcome prediction in patients with COVID-19, Radiology. (2021), 204141, https://doi.org/10.1148/radiol.2021204141.
[124] J.-W. Kim, J.S. Yoon, E.J. Kim, H.-L. Hong, H.H. Kwon, C.Y. Jung, K.C. Kim, Y. S. Sung, S.-H. Park, S.-K. Kim, J.-Y. Choe, Prognostic implication of baseline sarcopenia for length of hospital stay and survival in patients with coronavirus disease 2019, J. Gerontol. A. Biol. Sci. Med. Sci. (2021), https://doi.org/10.1093/gerona/glab085.
[125] F. Ufuk, M. Demirci, E. Sagtas, I.H. Akbudak, E. Ugurlu, T. Sari, The prognostic value of pneumonia severity score and pectoralis muscle Area on chest CT in adult COVID-19 patients, Eur. J. Radiol. 131 (2020), 109271, https://doi.org/10.1016/j.ejrad.2020.109271.
[126] S.A. Ritchie, J.M.C. Connell, The link between abdominal obesity, metabolic syndrome and cardiovascular disease, Nutr. Metab. Cardiovasc. Dis. 17 (2007) 319–326, https://doi.org/10.1016/j.numecd.2006.07.005.
[127] S.R. Smith, J.C. Lovejoy, F. Greenway, D. Ryan, L. deJonge, J. de la Bretonne, J. Volafova, G.A. Bray, Contributions of total body fat, abdominal subcutaneous adipose tissue compartments, and visceral adipose tissue to the metabolic complications of obesity, Metabolism. 50 (2001) 425–435, https://doi.org/10.1053/meta.2001.21693.
[128] H. Kwon, D. Kim, J.S. Kim, Body fat distribution and the risk of incident metabolic syndrome: a longitudinal cohort study, Sci. Rep. 7 (2017) 10955, https://doi.org/10.1038/s41598-017-09723-y.
[129] A.M. Kanaya, T. Harris, B.H. Goodpaster, F. Tylavsky, S.R. Cummings, Adipocytokines attenuate the association between visceral adiposity and diabetes in older adults, Diabetes Care. 27 (2004) 1375–1380, https://doi.org/10.2337/diacare.27.6.1375.
[130] J.F. Gautier, A. Mourier, E. de Kerviler, A. Tarentola, A.X. Bigard, J.M. Villette, C. Y. Guezennec, G. Cathelineau, Evaluation of abdominal fat distribution in noninsulin-dependent diabetes mellitus: relationship to insulin resistance, J. Clin. Endocrinol. Metab. 83 (1998) 1306–1311, https://doi.org/10.1210/jcem.83.4.4713.
[131] N. Covassin, F.H. Sert-Kuniyoshi, P. Singh, A. Romero-Corral, D.E. Davison, F. Lopez-Jimenez, M.D. Jensen, V.K. Somers, Experimental weight gain increases ambulatory blood pressure in healthy subjects: implications of visceral fat accumulation, Mayo Clin. Proc. 93 (2018) 618–626, https://doi.org/10.1016/j.mayocp.2017.12.012.
[132] G. Seravalle, G. Grassi, Obesity and hypertension, Pharmacol. Res. 122 (2017) 1–7, https://doi.org/10.1016/j.phrs.2017.05.013.
[133] H. Koh, T. Hayashi, K.K. Sato, N. Harita, I. Maeda, Y. Nishizawa, G. Endo, W. Y. Fujimoto, E.J. Boyko, Y. Hikita, Visceral adiposity, not abdominal subcutaneous fat area, is associated with high blood pressure in Japanese men: the Ohtori study, Hypertens. Res. 34 (2011) 565–572, https://doi.org/10.1038/hr.2010.271.
[134] Y. Matsuzawa, I. Shimomura, T. Nakamura, Y. Keno, K. Kotani, K. Tokunaga, Pathophysiology and pathogenesis of visceral fat obesity, Obes. Res. 3 (Suppl 2) (1995) 187S–194S, https://doi.org/10.1002/j.1550-8528.1995.tb00462.x.
[135] S.A. Lear, K.H. Humphries, S. Kohli, J.J. Frohlich, C.L. Birmingham, G.B. J. Mancini, Visceral adipose tissue, a potential risk factor for carotid atherosclerosis: results of the Multicultural Community Health Assessment Trial (M-CHAT), Stroke. 38 (2007) 2422–2429, https://doi.org/10.1161/STROKEAHA.107.484113.
[136] S.A. Lear, L.K. Sarna, T.J. Siow, G.B.J. Mancini, Y.L. Siow, K. O, Oxidative stress is associated with visceral adipose tissue and subclinical atherosclerosis in a healthy multi-ethnic population., Appl. Physiol. Nutr. Metab. = Physiol. Appl. Nutr. Metab. 37 (2012) 1164–1170. https://doi.org/10.1139/h2012-107.
[137] S. Lim, J.B. Meigs, Ectopic fat and cardiometabolic and vascular risk, Int. J. Cardiol. 169 (2013) 166–176, https://doi.org/10.1016/j.ijcard.2013.08.077.
[138] S.J. Kang, D. Km, H.E. Park, S.H. Choi, S.-Y. Choi, W. Lee, J.S. Kim, S.-H. Cho, Visceral adipose tissue area is associated with coronary stenosis and noncalcified plaques, Int. J. Obes. (Lond) 38 (2014) 272–278, https://doi.org/10.1038/ijo.2013.105.
[139] N. Ohashi, H. Yamamoto, J. Horiguchi, T. Kitagawa, E. Kunita, H. Utsunomiya, T. Oka, N. Kohno, Y. Kihara, Association between visceral adipose tissue area and coronary plaque morphology assessed by CT angiography, JACC. Cardiovasc. Imaging. 3 (2010) 908–917, https://doi.org/10.1016/j.jcmg.2010.06.014.
[140] T. Tanaka, S. Kishi, K. Ninomiya, D. Tomii, K. Koseki, Y. Sato, T. Okuno, K. Sato, H. Koike, K. Yahagi, K. Komiyama, J. Aoki, K. Tanabe, Impact of abdominal fat distribution, visceral fat, and subcutaneous fat on coronary plaque scores assessed by 320-row computed tomography coronary angiography, Atherosclerosis. 287 (2019) 155–161, https://doi.org/10.1016/j.atherosclerosis.2019.06.910.
[141] A. Engin, The definition and prevalence of obesity and metabolic syndrome, Adv. Exp. Med. Biol. 960 (2017) 1–17, https://doi.org/10.1007/978-3-319-48382-5_1.
[142] B. Mittal, Subcutaneous adipose tissue & visceral adipose tissue, Indian J. Med. Res. 149 (2019) 571–573, https://doi.org/10.4103/ijmr.IJMR_1910_18.
[143] R.V. Shah, V.L. Murthy, S.A. Abbasi, R. Blankstein, R.Y. Kwong, A.B. Goldfine, M. Jerosch-Herold, J.A.C. Lima, J. Ding, M.A. Allison, Visceral adiposity and the risk of metabolic syndrome across body mass index: the MESA Study, JACC. Cardiovasc. Imaging. 7 (2014) 1221–1235, https://doi.org/10.1016/j.jcmg.2014.07.017.
[144] A. Petersen, K. Bressem, J. Albrecht, H.-M. Thieß, J. Vahldiek, B. Hamm, M. R. Makowski, A. Niehues, S.M. Niehues, L.C. Adams, The role of visceral adiposity in the severity of COVID-19: Highlights from a unicenter cross-sectional pilot study in Germany, Metabolism. 110 (2020), 154317, https://doi.org/10.1016/j.metabol.2020.154317.
[145] F. Pediconi, V. Rizzo, S. Schiaffino, A. Cozzi, G. Della Pepa, F. Galati, C. Catalano, F. Sardanelli, Visceral adipose tissue area predicts intensive care unit admission in COVID-19 patients, Obes. Res. Clin. Pract. 15 (2021) 89–92, https://doi.org/10.1016/j.orcp.2020.12.002.
[146] H. Chandarana, B. Dane, A. Mikheev, M.T. Taffel, Y. Feng, H. Rusinek, Visceral adipose tissue in patients with COVID-19: risk stratification for severity, Abdom. Radiol. (New York) 46 (2021) 818–825, https://doi.org/10.1007/s00261-020-02693-2.
[147] A. Kalinkovich, G. Livshits, Sarcopenic obesity or obese sarcopenia: A cross talk between age-associated adipose tissue and skeletal muscle inflammation as a main mechanism of the pathogenesis, Ageing Res. Rev. 35 (2017) 200–221, https://doi.org/10.1016/j.arr.2016.09.008.
[148] K. Kohara, Sarcopenic obesity in aging population: current status and future directions for research, Endocrine. 45 (2014) 15–25, https://doi.org/10.1007/s12020-013-9992-0.
[149] L.M. Donini, L. Busetto, J.M. Bauer, S. Bischoff, Y. Boirie, T. Cederholm, A. J. Cruz-Jentoft, D. Dicker, G. Frühbeck, A. Giustina, M.C. Gonzalez, H.-S. Han, S. B. Heymsfield, T. Higashiguchi, A. Laviano, A. Lenzi, E. Parrinello, E. Poggiogalle, C.M. Prado, J.S. Rodriguez, Y. Rolland, F. Santini, M. Siervo, F. Tecilazich, R. Vettor, J. Yu, M. Zamboni, R. Barazzoni, Critical appraisal of definitions and diagnostic criteria for sarcopenic obesity based on a systematic review, Clin. Nutr. 39 (2020) 2368–2388, https://doi.org/10.1016/j.clnu.2019.11.024.
[150] C.M.M. Prado, J.R. Lieffers, L.J. McCargar, T. Reiman, M.B. Sawyer, L. Martin, V. E. Baracos, Prevalence and clinical implications of sarcopenic obesity in patients with solid tumours of the respiratory and gastrointestinal tracts: a population-based study, Lancet. Oncol. 9 (2008) 629–635, https://doi.org/10.1016/S1470-2045(08)70153-0.
[151] B.H.L. Tan, L.A. Birdsell, L. Martin, V.E. Baracos, K.C.H. Fearon, Sarcopenia in an overweight or obese patient is an adverse prognostic factor in pancreatic cancer, Clin. Cancer Res. 15 (2009) 6973–6979, https://doi.org/10.1158/1078-0432.CCR-09-1525.
[152] E.S. Gruber, G. Jomrich, D. Tamandl, M. Gnant, M. Schindl, K. Sahora, Sarcopenia and sarcopenic obesity are independent adverse prognostic factors in resectable pancreatic ductal adenocarcinoma, PLoS One. 14 (2019), https://doi.org/10.1371/journal.pone.0215915 e0215915–e0215915.
[153] S. Onishi, M. Tajika, T. Tanaka, K. Yamada, T. Abe, E. Higaki, T. Hosoi, Y. Inaba, K. Muro, M. Shimizu, Y. Niwa, Prognostic impact of sarcopenic obesity after neoadjuvant chemotherapy followed by surgery in elderly patients with esophageal squamous cell carcinoma, J Clin. Med. 9 (2020), https://doi.org/10.3390/jcm9092974.
[154] B.A. Grotenhuis, J. Shapiro, S. van Adrichem, M. de Vries, M. Koek, B.P. L. Wijnhoven, J.J.B. van Lanschot, Sarcopenia/muscle mass is not a prognostic factor for short- and long-term outcome after esophagectomy for cancer, World J. Surg. 40 (2016) 2698–2704, https://doi.org/10.1007/s00268-016-3603-1.
[155] J.S. Han, H. Ryu, I.J. Park, K.W. Kim, Y. Shin, S.O. Kim, S.-B. Lim, C.W. Kim, Y. S. Yoon, J.L. Lee, C.S. Yu, J.C. Kim, Association of body composition with long-term survival in non-metastatic rectal cancer patients, Cancer Res. Treat. 52 (2020) 563–572, https://doi.org/10.4143/crt.2019.249.
[156] M. Yamashita, K. Kamiya, A. Matsunaga, T. Kitamura, N. Hamazaki, R. Matsuzawa, K. Nozaki, S. Tanaka, T. Nakamura, E. Maekawa, T. Masuda, J. Ako, K. Miyaji, Prognostic value of sarcopenic obesity estimated by computed tomography in patients with cardiovascular disease and undergoing surgery, J. Cardiol. 74 (2019) 273–278, https://doi.org/10.1016/j.jjcc.2019.02.010.
[157] J.S. Oh, A.E. Ssentongo, P. Ssentongo, T. Dykes, L. Keeney, S.B. Armen, D. I. Soybel, Image-based assessment of sarcopenic obesity predicts mortality in major trauma, Am. J. Surg. (2021), https://doi.org/10.1016/j.amjsurg.2021.06.007.
[158] H.S. Sacks, J.N. Fain, Human epicardial adipose tissue: a review, Am. Heart J. 153 (2007) 907–917, https://doi.org/10.1016/j.ahj.2007.03.019.
[159] G. Iacobellis, Epicardial and pericardial fat: close, but very different., Obesity (Silver Spring). 17 (2009) 625; author reply 626-7. https://doi.org/10.1038/oby.2008.575.
[160] M. Guglielmo, A. Lin, D. Dey, A. Baggiano, L. Fusini, G. Muscogiuri, G. Pontone, Epicardial fat and coronary artery disease: role of cardiac imaging, Atherosclerosis. 321 (2021) 30–38, https://doi.org/10.1016/j.atherosclerosis.2021.02.008.
[161] G. Iacobellis, D. Corradi, A.M. Sharma, Epicardial adipose tissue: anatomic, biomolecular and clinical relationships with the heart, Nat. Clin. Pract. Cardiovasc. Med. 2 (2005) 536–543, https://doi.org/10.1038/ncpcardio0319.
[162] D. Dey, R. Nakazato, D. Li, D.S. Berman, Epicardial and thoracic fat - Noninvasive measurement and clinical implications, Cardiovasc. Diagn. Ther. 2 (2012) 85–93, https://doi.org/10.3978/j.issn.2223-3652.2012.04.03.
[163] J. Mancio, D. Azevedo, F. Saraiva, A.I. Azevedo, G. Pires-Morais, A. Leite-Moreira, I. Falcao-Pires, N. Lunet, N. Bettencourt, Epicardial adipose tissue volume assessed by computed tomography and coronary artery disease: a systematic review and meta-analysis, Eur. Hear. Journal. Cardiovasc. Imaging. 19 (2018) 490–497, https://doi.org/10.1093/ehjci/jex314.

[164] W. Zhu, H. Zhang, L. Guo, K. Hong, Relationship between epicardial adipose tissue volume and atrial fibrillation: a systematic review and meta-analysis, Herz. 41 (2016) 421–427, https://doi.org/10.1007/s00059-015-4387-z.
[165] Y. Higami, E. Ogawa, Y. Ryujin, K. Goto, R. Seto, H. Wada, N. Van Tho, L.T.T. Lan, P.D. Paré, Y. Nakano, Increased epicardial adipose tissue is associated with the airway dominant phenotype of chronic obstructive pulmonary disease, PLoS One. 11 (2016), e0148794, https://doi.org/10.1371/journal.pone.0148794.
[166] J. Zagaceta, J.J. Zulueta, G. Bastarrika, I. Colina, A.B. Alcaide, A. Campo, B. R. Celli, J.P. de Torres, Epicardial adipose tissue in patients with chronic obstructive pulmonary disease, PLoS One. 8 (2013), e65593, https://doi.org/10.1371/journal.pone.0065593.
[167] M. Deng, Y. Qi, L. Deng, H. Wang, Y. Xu, Z. Li, Z. Meng, J. Tang, Z. Dai, Obesity as a potential predictor of disease severity in young COVID-19 patients: a retrospective study, Obesity (Silver Spring). 28 (2020) 1815–1825, https://doi.org/10.1002/oby.22943.
[168] L. Slipczuk, F. Castagna, A. Schonberger, E. Novogrodsky, R. Sekerak, D. Dey, U. P. Jorde, J.M. Levsky, M.J. Garcia, Coronary artery calcification and epicardial adipose tissue as independent predictors of mortality in COVID-19, Int. J. Cardiovasc. Imaging. (2021), https://doi.org/10.1007/s10554-021-02276-2.
[169] K. Grodecki, A. Lin, A. Razipour, S. Cadet, P.A. McElhinney, C. Chan, B. D. Pressman, P. Julien, P. Maurovich-Horvat, N. Gaibazzi, U. Thakur, E. Mancini, C. Agalbato, R. Menè, G. Parati, F. Cernigliaro, N. Nerlekar, C. Torlasco, G. Pontone, P.J. Slomka, D. Dey, Epicardial adipose tissue is associated with extent of pneumonia and adverse outcomes in patients with COVID-19, Metabolism. 115 (2021), 154436, https://doi.org/10.1016/j.metabol.2020.154436.
[170] Z.-Y. Wei, R. Qiao, J. Chen, J. Huang, W.-J. Wang, H. Yu, J. Xu, H. Wu, C. Wang, C.-H. Gu, H.-J. Li, M. Li, C. Liu, J. Yang, H.-M. Ding, M.-J. Lu, W.-H. Yin, Y. Wang, K.-W. Li, H.-F. Shi, H.-Y. Qian, W.-X. Yang, Y.-J. Geng, Pre-existing health conditions and epicardial adipose tissue volume: potential risk factors for myocardial injury in COVID-19 patients, Front. Cardiovasc. Med. 7 (2020), 585220, https://doi.org/10.3389/fcvm.2020.585220.
[171] L. Slipczuk, F. Castagna, A. Schonberger, E. Novogrodsky, D. Dey, U.P. Jorde, J. M. Levsky, L. Di Biase, M.J. Garcia, Incidence of new-onset atrial fibrillation in COVID-19 is associated with increased epicardial adipose tissue, J. Interv. Card. Electrophysiol. Int. J. Arrhythm. Pacing. (2021) 1–9, https://doi.org/10.1007/s10840-021-01029-4.
[172] A. Abrishami, V. Eslami, Z. Baharvand, N. Khalili, S. Saghamanesh, E. Zarei, M. Sanei-Taheri, Epicardial adipose tissue, inflammatory biomarkers and COVID-19: Is there a possible relationship? Int. Immunopharmacol. 90 (2021), 107174 https://doi.org/10.1016/j.intimp.2020.107174.
[173] C. Conte, A. Esposito, R. De Lorenzo, L. Di Filippo, A. Palmisano, D. Vignale, R. Leone, V. Nicoletti, A. Ruggeri, G. Gallone, A. Secchi, E. Bosi, M. Tresoldi, A. Castagna, G. Landoni, A. Zangrillo, F. De Cobelli, F. Ciceri, P. Camici, P. Rovere-Querini, Epicardial adipose tissue characteristics, obesity and clinical outcomes in COVID-19: A post-hoc analysis of a prospective cohort study, Nutr. Metab. Cardiovasc. Dis. 31 (2021) 2156–2164, https://doi.org/10.1016/j.numecd.2021.04.020.
[174] K. Shibata, M. Yamamoto, S. Yamada, T. Kobayashi, S. Morita, A. Kagase, T. Tokuda, T. Shimura, T. Tsunaki, N. Tada, T. Naganuma, M. Araki, F. Yamanaka, S. Shirai, K. Mizutani, M. Tabata, H. Ueno, K. Takagi, A. Higashimori, Y. Watanabe, K. Hayashida, Clinical outcomes of subcutaneous and visceral adipose tissue characteristics assessed in patients underwent transcatheter aortic valve replacement, CJC Open. 3 (2021) 142–151, https://doi.org/10.1016/j.cjco.2020.09.019.
[175] G. Kim, J.H. Kim, Impact of skeletal muscle mass on metabolic health, Endocrinol. Metab. (Seoul, Korea). 35 (2020) 1–6, https://doi.org/10.3803/EnM.2020.35.1.1.
[176] M. Tanaka, H. Okada, Y. Hashimoto, M. Kumagai, H. Nishimura, Y. Oda, M. Fukui, Relationship between metabolic syndrome and trunk muscle quality as well as quantity evaluated by computed tomography, Clin. Nutr. 39 (2020) 1818–1825, https://doi.org/10.1016/j.clnu.2019.07.021.
[177] C.A. Vella, M.C. Nelson, J.T. Unkart, I. Miljkovic, M.A. Allison, Skeletal muscle area and density are associated with lipid and lipoprotein cholesterol levels: the Multi-Ethnic Study of Atherosclerosis, J. Clin. Lipidol. 14 (2020) 143–153, https://doi.org/10.1016/j.jacl.2020.01.002.
[178] J. Ding, S.B. Kritchevsky, F.-C. Hsu, T.B. Harris, G.L. Burke, R.C. Detrano, M. Szklo, M.H. Criqui, M. Allison, P. Ouyang, E.R. Brown, J.J. Carr, Association between non-subcutaneous adiposity and calcified coronary plaque: a substudy of the Multi-Ethnic Study of Atherosclerosis, Am. J. Clin. Nutr. 88 (2008) 645–650, https://doi.org/10.1093/ajcn/88.3.645.
[179] S.W. Moon, J.S. Choi, S.H. Lee, K.S. Jung, J.Y. Jung, Y.A. Kang, M.S. Park, Y. S. Kim, J. Chang, S.Y. Kim, Thoracic skeletal muscle quantification: low muscle mass is related with worse prognosis in idiopathic pulmonary fibrosis patients, Respir. Res. 20 (2019) 35, https://doi.org/10.1186/s12931-019-1001-6.
[180] A. Nakano, H. Ohkubo, H. Taniguchi, Y. Kondoh, T. Matsuda, M. Yagi, T. Furukawa, Y. Kanemitsu, A. Niimi, Early decrease in erector spinae muscle area and future risk of mortality in idiopathic pulmonary fibrosis, Sci. Rep. 10 (2020) 2312, https://doi.org/10.1038/s41598-020-59100-5.
[181] . Pishgar, M. Shabani, T. Quinaglia A C Silva, D.A. Bluemke, M. Budoff, R.G. Barr, M.A. Allison, W.S. Post, J.A.C. Lima, S. Demehri, Quantitative Analysis of Adipose Depots by Using Chest CT and Associations with All-Cause Mortality in Chronic Obstructive Pulmonary Disease: Longitudinal Analysis from MESArthritis Ancillary Study., Radiology. (2021) 203959. https://doi.org/10.1148/radiol.2021203959.
[182] J. Kim, K.-H. Choi, S.-G. Cho, S.-R. Kang, S.W. Yoo, S.Y. Kwon, J.-J. Min, H.-S. Bom, H.-C. Song, Association of muscle and visceral adipose tissues with the probability of Alzheimer's disease in healthy subjects, Sci. Rep. 9 (2019) 949, https://doi.org/10.1038/s41598-018-37244-9.
[183] C. Tanabe, M.J. Reed, T.N. Pham, K. Penn, I. Bentov, S.J. Kaplan, Association of brain atrophy and masseter sarcopenia with 1-year mortality in older trauma patients, JAMA Surg. 154 (2019) 716–723, https://doi.org/10.1001/jamasurg.2019.0988.
[184] K. Shibahashi, K. Sugiyama, H. Hoda, Y. Hamabe, Skeletal muscle as a factor contributing to better stratification of older patients with traumatic brain injury: a retrospective cohort study, World Neurosurg. 106 (2017) 589–594, https://doi.org/10.1016/j.wneu.2017.07.025.
[185] A. Kumar, M.R. Moynagh, F. Multinu, W.A. Cliby, M.E. McGree, A.L. Weaver, P. M. Young, J.N. Bakkum-Gamez, C.L. Langstraat, S.C. Dowdy, A. Jatoi, A. Mariani, Muscle composition measured by CT scan is a measurable predictor of overall survival in advanced ovarian cancer, Gynecol. Oncol. 142 (2016) 311–316, https://doi.org/10.1016/j.ygyno.2016.05.027.
[186] S.-A.M. Staley, K. Tucker, J. Oldan, D.T. Moore, M. Newton, M. Ertel, L. West, V. Bae-Jump, Visceral adiposity as a predictor of survival in patients with epithelial ovarian cancer receiving platinum and taxane-based chemotherapy, e17031 e17031, J. Clin. Oncol. 37 (2019), https://doi.org/10.1200/JCO.2019.37.15_suppl.e17031.
[187] M.L. Torres, L.C. Hartmann, W.A. Cliby, K.R. Kalli, P.M. Young, A.L. Weaver, C. L. Langstraat, A. Jatoi, S. Kumar, A. Mariani, Nutritional status, CT body composition measures and survival in ovarian cancer, Gynecol. Oncol. 129 (2013) 548–553, https://doi.org/10.1016/j.ygyno.2013.03.003.
[188] N. Yoshikawa, A. Shirakawa, K. Yoshida, S. Tamauchi, S. Suzuki, F. Kikkawa, H. Kajiyama, Sarcopenia as a predictor of survival among patients with organ metastatic cervical cancer, Nutr. Clin. Pract. Off. Publ. Am. Soc. Parenter. Enter. Nutr. 35 (2020) 1041–1046, https://doi.org/10.1002/ncp.10482.
[189] M.A. Franzoi, C. Vandeputte, D. Eiger, R. Caparica, M. Brandão, C. De Angelis, A. Hendlisz, A. Awada, M. Piccart, E. de Azambuja, Computed tomography-based analyses of baseline body composition parameters and changes in breast cancer patients under treatment with CDK 4/6 inhibitors, Breast Cancer Res. Treat. 181 (2020) 199–209, https://doi.org/10.1007/s10549-020-05617-2.
[190] A. Okamura, M. Watanabe, K. Yamashita, M. Yuda, M. Hayami, Y. Imamura, S. Mine, Implication of visceral obesity in patients with esophageal squamous cell carcinoma, Langenbeck's Arch. Surg. 403 (2018) 245–253, https://doi.org/10.1007/s00423-017-1643-0.
[191] X.-T. Li, L. Tang, Y. Chen, Y.-L. Li, X.-P. Zhang, Y.-S. Sun, Visceral and subcutaneous fat as new independent predictive factors of survival in locally advanced gastric carcinoma patients treated with neo-adjuvant chemotherapy, J. Cancer Res. Clin. Oncol. 141 (2015) 1237–1247, https://doi.org/10.1007/s00432-014-1893-y.
[192] M. Shirdel, F. Andersson, R. Myte, J. Axelsson, M. Rutegård, L. Blomqvist, K. Riklund, B. van Guelpen, R. Palmqvist, B. Gylling, Body composition measured by computed tomography is associated with colorectal cancer survival, also in early-stage disease, Acta Oncol. 59 (2020) 799–808, https://doi.org/10.1080/0284186X.2020.1744716.
[193] L. Thoresen, G. Frykholm, S. Lydersen, H. Ulveland, V. Baracos, C.M.M. Prado, L. Birdsell, U. Falkmer, Nutritional status, cachexia and survival in patients with advanced colorectal carcinoma. Different assessment criteria for nutritional status provide unequal results, Clin. Nutr. 32 (2013) 65–72, https://doi.org/10.1016/j.clnu.2012.05.009.
[194] D. Basile, M. Bartoletti, M. Polano, L. Bortot, L. Gerratana, P. Di Nardo, M. Borghi, V. Fanotto, G. Pelizzari, C. Lisanti, M. Garutti, S. Buriolla, E. Ongaro, E. Andreuzzi, M. Montico, L. Balestreri, G. Miolo, G. Toffoli, G. Aprile, F. Puglisi, A. Buonadonna, Prognostic role of visceral fat for overall survival in metastatic colorectal cancer: a pilot study, Clin. Nutr. 40 (2021) 286–294, https://doi.org/10.1016/j.clnu.2020.05.019.
[195] D.P.J. van Dijk, M.J.A.M. Bakens, M.M.E. Coolsen, S.S. Rensen, R.M. van Dam, M. J.L. Bours, M.P. Weijenberg, C.H.C. Dejong, S.W.M. Olde Damink, Low skeletal muscle radiation attenuation and visceral adiposity are associated with overall survival and surgical site infections in patients with pancreatic cancer, J. Cachexia. Sarcopenia Muscle. 8 (2017) 317–326, https://doi.org/10.1002/jcsm.12155.
[196] K.M. Di Sebastiano, L. Yang, K. Zbuk, R.K. Wong, T. Chow, D. Koff, G.R. Moran, M. Mourtzakis, Accelerated muscle and adipose tissue loss may predict survival in pancreatic cancer patients: the relationship with diabetes and anaemia, Br. J. Nutr. 109 (2013) 302–312, https://doi.org/10.1017/S0007114512001067.
[197] J. Nattenmüller, R. Wochner, T. Muley, M. Steins, S. Hummler, B. Teucher, J. Wiskemann, H.-U. Kauczor, M.O. Wielpütz, C.P. Heussel, Prognostic impact of CT-quantified muscle and fat distribution before and after first-line-chemotherapy in lung cancer patients, PLoS One. 12 (2017), e0169136, https://doi.org/10.1371/journal.pone.0169136.
[198] M.G. Vitale, D. Basile, E. Bertoli, M. Giavarra, G. Pelizzari, L. Palmero, D. Zara, G. Targato, G. Pascoletti, M. Cinausero, E. Poletto, D. Iacono, F. Puglisi, G. Fasola, A.M. Minisini, 1367P - Impact of sarcopenia in patients with metastatic melanoma treated with immunotherapy, Ann. Oncol. 30 (2019), https://doi.org/10.1093/annonc/mdz255.055.
[199] V.P. Grignol, A.D. Smith, D. Shlapak, X. Zhang, S.M. Del Campo, W.E. Carson, Increased visceral to subcutaneous fat ratio is associated with decreased overall survival in patients with metastatic melanoma receiving anti-angiogenic therapy, Surg. Oncol. 24 (2015) 353–358, https://doi.org/10.1016/j.suronc.2015.09.002.
[200] A.R. Jung, J.-L. Roh, J.S. Kim, S.-B. Kim, S.-H. Choi, S.Y. Nam, S.Y. Kim, Prognostic value of body composition on recurrence and survival of advanced-

stage head and neck cancer, Eur. J. Cancer. 116 (2019) 98–106, https://doi.org/10.1016/j.ejca.2019.05.006.
[201] A.J. Grossberg, S. Chamchod, C.D. Fuller, A.S.R. Mohamed, J. Heukelom, H. Eichelberger, M.E. Kantor, K.A. Hutcheson, G.B. Gunn, A.S. Garden, S. Frank, J. Phan, B. Beadle, H.D. Skinner, W.H. Morrison, D.I. Rosenthal, Association of body composition with survival and locoregional control of radiotherapy-treated head and neck squamous cell carcinoma, JAMA Oncol. 2 (2016) 782–789, https://doi.org/10.1001/jamaoncol.2015.6339.
[202] Y. Choi, K.-J. Ahn, J. Jang, N.-Y. Shin, S.-L. Jung, B.-S. Kim, M.-S. Kim, Y.-S. Kim, Prognostic value of computed tomography-based volumetric body composition analysis in patients with head and neck cancer: feasibility study, Head Neck. 42 (2020) 2614–2625, https://doi.org/10.1002/hed.26310.
[203] K.A. Philbrick, A.D. Weston, Z. Akkus, T.L. Kline, P. Korfiatis, T. Sakinis, P. Kostandy, A. Boonrod, A. Zeinoddini, N. Takahashi, B.J. Erickson, RIL-contour: a medical imaging dataset annotation tool for and with deep learning, J. Digit. Imaging. 32 (2019) 571–581, https://doi.org/10.1007/s10278-019-00232-0.
[204] iTomography Corporation, Medical CT Imaging software, (n.d.). https://radsource.us/protonpacs-pacs/.
[205] Siemens hleathineer, Syngo.via, (n.d.). https://www.siemens-healthineers.com/co/medical-imaging-it/clinical-imaging-applications/syngovia.